PHYSICAL REVIEW D **88,** 015014 (2013)

$SO(10)$ inspired gauge-mediated supersymmetry breaking

M. E. Krauss* and W. Porod†

Institut für Theoretische Physik und Astronomie, Universität Würzburg, Am Hubland, 97074 Würzburg, Germany

F. Staub‡

Bethe Center for Theoretical Physics and Physikalisches Institut der Universität Bonn, 53115 Bonn, Germany

(Received 8 April 2013; published 10 July 2013)

We consider a supersymmetric model motivated by a $SO(10)$ grand unified theory: the gauge sector near the supersymmetry scale consists of $SU(3)_c \times SU(2)_L \times U(1)_R \times U(1)_{B-L}$. We embed this model in minimal gauge mediation and incorporate neutrino data via an inverse seesaw mechanism. Also in this restricted model, the additional D terms can raise the light Higgs mass in a sizable way. Therefore, it is much easier to obtain $m_h \simeq 125$ GeV without the need to push the supersymmetry spectrum to extremely large values as it happens in models with minimal supersymmetric standard model particle content only. We show that this model predicts a diphoton rate of the Higgs equal to or smaller than the standard model expectation. We discuss briefly the collider phenomenology with a particular focus on the next to lightest supersymmetric particle in which this model offers the sneutrino as an additional possiblity. Moreover, we point out that, also in this model variant, supersymmetry can be discovered in Z' decays even in scenarios in which the strongly interacting particles are too heavy to be produced at a sizable rate at the LHC with 14 TeV. In addition, we show that lepton flavor violating observables constrain the size of the neutrino Yukawa couplings for which, in particular, muon decays and $\mu - e$ conversion in heavy atoms are of particular importance. Once these constraints are fulfilled, the rates for τ decays are predicted to be below the reach of near-future experiments.

DOI: 10.1103/PhysRevD.88.015014 PACS numbers: 12.60.Jv, 12.60.Cn, 14.80.Da, 14.70.Pw

I. INTRODUCTION

The LHC is rapidly extending our knowledge of the TeV scale. However, there is currently no hint of new physics beyond the standard model (SM), which leads to severe lower limits on the mass of new, especially colored, particles. One of the most popular model classes to extend the SM is supersymmetry (SUSY), in particular, the minimal supersymmetric standard model (MSSM). As the MSSM itself has over 100 free parameters, which are mainly part of the SUSY breaking sector, mechanisms of SUSY breaking, which depend only on a few parameters and which predict distinct relations among the different soft terms, have been studied. Those models trigger SUSY breaking in our visible sector by communicating with a hidden sector in which SUSY gets broken at the first place. Popular mechanisms of transmitting SUSY breaking from the hidden to the visible sector work either via gravity like in supergravity [1,2] or via gauge interactions with so-called messenger fields like in gauge-mediated supersymmetry breaking (GMSB) [3–11] with six parameters. GMSB has the appealing feature that it is a flavor blind SUSY breaking. Hence, it solves automatically the flavor problem if the SUSY breaking scale is not too high. In addition, the gravitino is the lightest supersymmetric particle (LSP) and usually the dark matter candidate in this kind of models.

However, both models are under big pressure because of the observation of a SM-like Higgs boson with mass of 125 GeV [12,13]. Even if this mass is below the absolute upper limit of about 132 GeV, which can be reached for the light Higgs mass in the most general MSSM [14], it is already very hard to explain it in the constrained MSSM with five parameters [15–17] and demands large SUSY breaking masses and especially a large mass splitting in the stop sector. This mass splitting is caused by large trilinear couplings. However, in GMSB, these terms are always small even if the μ/B_μ problem of the GMSB is solved [18]. That makes it even more difficult to obtain a Higgs mass in the correct range [19]. This caused increasing interest in nonminimal GMSB models, which involve also superpotential interactions between the matter and messenger sector to create large trilinear terms [20–29].

Another possibility to reduce this tension between the Higgs mass and the simplest constrained models is to extend the Higgs sector of the MSSM. The smallest possible extension is to add a gauge singlet like in the next-to-minimal supersymmetric standard model (NMSSM) (see Refs. [30,31] and references therein). The singlet and the corresponding superpotential coupling to the Higgs doublets can significantly lift the upper limit on the light Higgs mass of $m_h < M_Z$ at tree level in the MSSM by new F-term contributions [32]. It has been shown that, even in the constrained NMSSM, a Higgs

*manuel.krauss@physik.uni-wuerzburg.de
†porod@physik.uni-wuerzburg.de
‡fnstaub@th.physik.uni-bonn.de

mass of 125 GeV can be explained [33,34]. If one drops in addition the assumption of a Z_3 symmetry and considers instead the generalized NMSSM, these masses are obtained with even less fine-tuning [35]. The same feature can also be observed in models with Dirac instead of Majorana gauginos which usually come with an extended Higgs sector [36]. There are also some hints that the branching ratio of the observed particles do not completely agree with the SM expectations. In particular, the diphoton rate seems to be enhanced, which is usually hard to explain in the context of the (constrained) MSSM [37,38]. In contrast, this enhancement can much more easily be obtained in the NMSSM or its generalized version [33,39–43].

A second possibility is to consider models with extended gauge structures, which arise naturally in the context of embedding the SM gauge group in a larger group such as $SO(10)$ or E_6; see, e.g., Refs. [44–49]. In those models, the upper bound on the lightest Higgs boson is also relaxed, this time due to additional D-term contributions [50–55]. Furthermore, they often provide the possibility to explain neutrino data: either via seesaw types I–III, which involve heavy states [56–59], or via an inverse or linear seesaw with additional matter fields at the SUSY scale [60–62]. Another interesting feature is that such models can also have a new gauge boson (Z') with a mass in the TeV range [63,64]. Hence, intensive searches for Z' bosons have been performed, and bounds on their mass have been set [65–68]. For reviews on various Z' models, see, e.g., Refs. [69,70].

In addition, $U(1)$ extensions of the SM provide another peculiar feature, which can have very interesting effects, namely, gauge kinetic mixing [71–73]. While gauge kinetic mixing is often ignored in phenomenological studies, it has been shown recently in several works that it can have a significant effect on Z' phenomenology [74–76] but also on the Higgs mass [77] and dark matter properties [78,79].

In this work, we will assume minimal GMSB inspired by $SO(10)$: the grand unified theory (GUT) group gets broken to $SU(3)_c \times SU(2)_L \times U(1)_R \times U(1)_{B-L}$ very close to the GUT scale but well above the scale of the messenger fields that trigger GMSB. In contrast to previous studies, we assume, however, that the breaking down to the SM gauge groups takes place at the TeV scale, i.e., well below the lowest messenger scale. Hence, we study a messenger sector charged under $U(1)_R \times U(1)_{B-L}$, which will change our boundary conditions. Furthermore, we gain an enhancement of the mass of the light Higgs boson. In addition, we follow the setup of Ref. [80], in which this model has been studied in gravity mediation, and assume additional gauge singlets present at the SUSY scale to incorporate neutrino masses and mixing via the inverse seesaw.

The remainder of this paper is organized as follows. In Sec. II, we briefly summarize the main features of the model and its particle content. In Sec. III, we discuss the results for Higgs physics under consideration, check the bounds coming from lepton flavor violation (LFV) observables on the model parameters, and comment on the expected collider phenomenology. We conclude in Sec. IV.

II. ASPECTS OF THE MODEL

A. Particle content and superpotential

In this section, we discuss briefly the particle content and the superpotential of the model under consideration. For a detailed discussion of the particle spectrum, we refer to Refs. [55,80]. The superpotential is given by

$$\begin{aligned}\mathcal{W} = {} & Y_u^{ij}\hat{u}_i^c\hat{Q}_j\hat{H}_u - Y_d^{ij}\hat{d}_i^c\hat{Q}_j\hat{H}_d - Y_e^{ij}\hat{e}_i^c\hat{L}_j\hat{H}_d + \mu\hat{H}_u\hat{H}_d \\ & + Y_\nu^{ij}\hat{\nu}_i^c\hat{L}_j\hat{H}_u + Y_S^{ij}\hat{\nu}_i^c\hat{S}_j\hat{\chi}_R - \mu_R\hat{\bar{\chi}}_R\hat{\chi}_R + \mu_S^{ij}\hat{S}_i\hat{S}_j,\end{aligned} \tag{1}$$

where the upper line corresponds to the standard MSSM superpotential, and the lower line contains the new sector as well as the ingredients for the inverse seesaw mechanism: Y_S and Y_ν being the neutrino Yukawa couplings and μ_S the mass term for the singlet field S, which is responsible for the mass of the light neutrinos. In Sec. II D, we will see that this model with an inverse seesaw mechanism for neutrinos is much easier to implement in GMSB than the corresponding model with the type I seesaw in which the $\hat{S}_i$ fields are absent.

The scalar fields χ_R and $\bar{\chi}_R$ break $U(1)_R \times U(1)_{B-L}$ down to $U(1)_Y$. As we interpret the $B-L$ charge of these fields as a lepton number, this leads to a spontaneous breaking of the usual R parity. Moreover, the usual R parity would allow additional terms in the superpotential such as $\hat{\bar{\chi}}_R\hat{L}_j\hat{H}_u$, which also contribute to this breaking as soon as electroweak symmetry is broken. To avoid this, we introduce a Z_2^M matter parity as it has also been proposed in Refs. [81,82] in similar frameworks. Under this parity, $\hat{H}_d$, $\hat{H}_u$, $\hat{\chi}_R$, and $\hat{\bar{\chi}}_R$ are even, and all other fields are odd. We have checked that in this way also the contraints due to the so-called discrete gauge symmetry anomalies are fulfilled [83,84]. For completeness, we note that this symmetry is sufficient to forbid the dangerous terms leading to proton decay, which is the main purpose of the usual R parity. Moreover, also, the stability of the lightest supersymmetric particle is ensured in this way.

Interestingly, the particle content of this model is in agreement with gauge coupling unification even if the breaking scale of $SU(3)_c \times SU(2)_L \times U(1)_R \times U(1)_{B-L} \to SU(3)_c \times SU(2)_L \times U(1)_Y$ is close to the breaking scale down to $SU(3)_c \times U(1)_{em}$. Therefore, we will always assume a one-step breaking $SU(3)_c \times SU(2)_L \times U(1)_R \times U(1)_{B-L} \to SU(3)_c \times U(1)_{em}$ in the following. However, to facilitate the comparison with the MSSM, we will work in a different basis for the $U(1)$ sector: we will take $U(1)_Y \times U(1)_\chi$ as the orthogonal basis instead of

TABLE I. Chiral superfields and their quantum numbers with respect to $SU(3)_c \times SU(2)_L \times U(1)_R \times U(1)_{B-L}$. We also give the quantum numbers in the basis $SU(3)_c \times SU(2)_L \times U(1)_Y \times U(1)_\chi$, the relations between both bases is defined in Sec. II B.

Superfield	Spin 0	Spin $\frac{1}{2}$	Generations	$SU(3)_c \times SU(2)_L$	$U(1)_R \times U(1)_{B-L}$	$U(1)_Y \times U(1)_\chi$
$\hat{Q}$	$\tilde{Q}$	Q	3	$(\mathbf{3}, \mathbf{2})$	$(0, \frac{1}{6})$	$(\frac{1}{6}, \frac{1}{4})$
$\hat{d}^c$	$\tilde{d}^c$	d^c	3	$(\bar{\mathbf{3}}, \mathbf{1})$	$(\frac{1}{2}, -\frac{1}{6})$	$(\frac{1}{3}, -\frac{3}{4})$
$\hat{u}^c$	$\tilde{u}^c$	u^c	3	$(\bar{\mathbf{3}}, \mathbf{1})$	$(-\frac{1}{2}, -\frac{1}{6})$	$(-\frac{2}{3}, \frac{1}{4})$
$\hat{L}$	$\tilde{L}$	L	3	$(\mathbf{1}, \mathbf{2})$	$(0, -\frac{1}{2})$	$(-\frac{1}{2}, -\frac{3}{4})$
$\hat{e}^c$	$\tilde{e}^c$	e^c	3	$(\mathbf{1}, \mathbf{1})$	$(\frac{1}{2}, \frac{1}{2})$	$(1, \frac{1}{4})$
$\hat{\nu}^c$	$\tilde{\nu}^c$	ν^c	3	$(\mathbf{1}, \mathbf{1})$	$(-\frac{1}{2}, \frac{1}{2})$	$(0, \frac{5}{4})$
$\hat{S}$	$\tilde{S}$	S	3	$(\mathbf{1}, \mathbf{1})$	$(0, 0)$	$(0, 0)$
$\hat{H}_d$	H_d	$\tilde{H}_d$	1	$(\mathbf{1}, \mathbf{2})$	$(-\frac{1}{2}, 0)$	$(-\frac{1}{2}, \frac{1}{2})$
$\hat{H}_u$	H_u	$\tilde{H}_u$	1	$(\mathbf{1}, \mathbf{2})$	$(\frac{1}{2}, 0)$	$(\frac{1}{2}, -\frac{1}{2})$
$\hat{\chi}_R$	χ_R	$\tilde{\chi}_R$	1	$(\mathbf{1}, \mathbf{1})$	$(\frac{1}{2}, -\frac{1}{2})$	$(0, -\frac{5}{4})$
$\hat{\bar{\chi}}_R$	$\bar{\chi}_R$	$\tilde{\bar{\chi}}_R$	1	$(\mathbf{1}, \mathbf{1})$	$(-\frac{1}{2}, \frac{1}{2})$	$(0, \frac{5}{4})$

$U(1)_R \times U(1)_{B-L}$. We give the corresponding $U(1)$ quantum numbers for both bases in Table I.

The soft SUSY breaking terms are

$$\begin{aligned}\mathcal{V}_{\text{soft}} = m_{ij}^2 \phi_i^* \phi_j + \Big(&\frac{1}{2} M_{ab} \lambda_a \lambda_b + B_\mu H_u H_d + B_{\mu_R} \bar{\chi}_R \chi_R \\ &+ B_{\mu_S} \tilde{S} \tilde{S} + T_d^{ij} H_d \tilde{d}_i^c \tilde{Q}_j + T_u^{ij} H_u \tilde{u}_i^c \tilde{Q}_j + T_e^{ij} H_d \tilde{e}_i^c \tilde{L}_j \\ &+ T_\nu^{ij} H_u \tilde{\nu}_i^c \tilde{L}_j + T_S^{ij} \chi_R \tilde{\nu}_i^c \tilde{S}_j + \text{H.c.}\Big),\end{aligned} \tag{2}$$

with the generation indices i and j. We have introduced here ϕ_i for all scalar particles and λ_a for the different gauginos. Note that, because of the two Abelian gauge groups present in the model and the consequential gauge kinetic mixing discussed in Sec. II B, also the mixed soft gaugino term $M_{Y\chi} \lambda_Y \lambda_\chi$ is present [85].

B. Gauge kinetic mixing

Even if $U(1)_R$ and $U(1)_{B-L}$ can be embedded orthogonal in $SO(10)$ at a given scale, a kinetic mixing term of the form

$$\mathcal{L}_{\text{mix}} = -\chi F^{B-L,\mu\nu} F^R_{\mu\nu} \tag{3}$$

can occur. The reason is that the Higgs fields we assume to be present at the SUSY scale do not form a complete representation of $SO(10)$. Hence, kinetic mixing will be introduced by renormalization group equation (RGE) evolution. This can be seen by the off-diagonal elements of the anomalous dimension matrix, which in the basis $(U(1)_R, U(1)_{B-L})$ at one loop is given by

$$\gamma = \frac{1}{16\pi^2} N \begin{pmatrix} \frac{15}{2} & \frac{1}{2} \\ \frac{1}{2} & \frac{9}{2} \end{pmatrix} N. \tag{4}$$

Here, $N = \text{diag}(1, \sqrt{3/2})$ contains the GUT normalization. In order to correctly account for gauge kinetic mixing effects, we follow the approach given in Ref. [85] and shift the term to a covariant derivative of the form

$$D^\mu = \partial^\mu - i Q_l G_{lm} A_m^\mu, \tag{5}$$

where

$$G = \begin{pmatrix} g_R & g_{RBL} \\ g_{BLR} & g_{BL} \end{pmatrix}, \tag{6}$$

$A^\mu = (A_R^\mu, A_{B-L}^\mu)^T$ and Q is a vector containing the $U(1)$ charges of the field under consideration. We assume the breaking into $U(1)_R \times U(1)_{B-L}$ to take place at the GUT scale M_{GUT} and demand $g_{RBL} = g_{\text{BLR}} = 0$ at M_{GUT} as the initial condition. In addition, we have the freedom to go into a particular basis by rotating the gauge bosons of the Abelian groups. As already mentioned, for an easier comparison with the usual GMSB, we take the basis $U(1)_Y \times U(1)_\chi$ for which the first factor is the usual hypercharge and the second one is the orthogonal one within $SO(10)$. The gauge couplings and charges of $U(1)_R \times U(1)_{B-L}$ and $U(1)_Y \times U(1)_\chi$ are (without GUT normalization) related via

$$\begin{aligned} A^\mu \to A'^\mu = \begin{pmatrix} A_Y^\mu \\ A_\chi^\mu \end{pmatrix}, \qquad Q \to Q' = \begin{pmatrix} q_{B-L} + q_R \\ \frac{3}{2} q_{B-L} - q_R \end{pmatrix}, \\ G \to G' = \begin{pmatrix} g_Y & g_{Y\chi} \\ 0 & g_\chi \end{pmatrix}, \end{aligned} \tag{7}$$

with

$$\begin{aligned} g_Y &= \frac{g_{BL} g_R - g_{BLR} g_{RBL}}{\sqrt{(g_{BLR} - g_R)^2 + (g_{BL} - g_{RBL})^2}}, \\ g_\chi &= \frac{2}{5} \sqrt{(g_{BLR} - g_R)^2 + (g_{BL} - g_{RBL})^2}, \\ g_{Y\chi} &= \frac{2(g_{BL}^2 + g_{BLR}^2) + g_{BLR} g_R + g_{BL} g_{RBL} - 3(g_R^2 + g_{RBL}^2)}{5\sqrt{(g_{BLR} - g_R)^2 + (g_{BL} - g_{RBL})^2}}. \end{aligned} \tag{8}$$

C. GMSB boundary conditions

In GMSB models, it is assumed that supersymmetry breaking is generated by one or more superfields $\hat{X}_k$ living in a "secluded" sector. We assume for simplicity that only one field $\hat{X}$ is present, which is coupled to a set of messenger superfields $\hat{\Phi}_i$ via

$$\mathcal{W}_{\rm GM} = \lambda_i \hat{X} \hat{\Phi}_i \hat{\bar{\Phi}}_i. \tag{9}$$

Furthermore, it is assumed that the scalar and auxiliary components of X receive a vacuum expectation value (VEV),

$$\langle X \rangle = M + \theta^2 F, \tag{10}$$

and that it couples universally to $\hat{\Phi}_i$, implying that one can set $\lambda_i = 1$. The supersymmetry breaking due to the F-term VEV is communicated to the visible sector via the gauge interactions of the Φ_i. Since we are interested in minimal gauge mediation without spoiling gauge coupling unification, we assume that the messenger fields form a complete $SO(10)$ multiplet, e.g., a **10**-plet. This results in two $SU(2)_L$ doublets and two $SU(3)_c$ triplets below the $SO(10)$ scale with suitable charges under the Abelian gauge groups, which are listed in Table II.

The SUSY breaking gaugino and scalar masses are generated via 1- and 2-loop diagrams, respectively [86–89]. Neglecting gauge kinetic mixing, the boundary conditions for the SUSY breaking masses are given by [88]

$$M_a = \frac{g_a^2}{16\pi^2} \Lambda \sum_i n_a(i) g(x_i), \tag{11}$$

$$m_k^2 = 2\Lambda^2 \sum_a C_a(k) \frac{g_a^4}{(16\pi^2)^2} \sum_i n_a(i) f(x_i), \tag{12}$$

with $\Lambda = F/M$, $x_i = |\Lambda/M|$, and $g(x)$ and $f(x)$ are approximately 1 for $x \lesssim 0.2$. g_a denotes the coupling of gauge group a, and i runs over the messenger fields. $n_a(i)$ is the Dynkin index of the messenger with respect to the gauge group i. We use a normalization in which $n_a = 1$ for the **10** of $SO(10)$. $C_a(k)$ is the quadratic Casimir invariant of the scalar field k.

For a proper treatment of gauge kinetic mixing, we use the substitution rules for Abelian groups given in Ref. [85].

TABLE II. Quantum numbers of the messenger fields in the respective bases.

	$SU(3)_c \times SU(2)_L$	$U(1)_R \times U(1)_{B-L}$	$U(1)_Y \times U(1)_\chi$
$\hat{\Phi}_1$	$(\mathbf{1}, \mathbf{2})$	$(\frac{1}{2}, 0)$	$(\frac{1}{2}, -\frac{1}{2})$
$\hat{\bar{\Phi}}_1$	$(\mathbf{1}, \mathbf{2})$	$(-\frac{1}{2}, 0)$	$(-\frac{1}{2}, \frac{1}{2})$
$\hat{\Phi}_2$	$(\mathbf{3}, \mathbf{1})$	$(0, -\frac{1}{3})$	$(-\frac{1}{3}, -\frac{1}{2})$
$\hat{\bar{\Phi}}_2$	$(\bar{\mathbf{3}}, \mathbf{1})$	$(0, \frac{1}{3})$	$(\frac{1}{3}, \frac{1}{2})$

The resulting soft masses for the gauginos and scalars at the messenger scale read

$$M_{A \neq \text{Abelian}} = \frac{g_A^2}{16\pi^2} \Lambda \sum_i n_A(i) g(x_i), \tag{13}$$

$$M_{kl=\text{Abelian}} = \frac{1}{16\pi^2} \Lambda \left(\sum_i g(x_i) G^T N Q_i Q_i^T N G \right)_{kl}, \tag{14}$$

$$m_k^2 = \frac{2}{(16\pi^2)^2} \Lambda^2 \Bigg(\sum_{A \neq \text{Abelian}} C_A(k) g_A^4 \sum_i f(x_i) n_A(i) + \sum_i f(x_i) (Q_k^T N G G^T N Q_i)^2 \Bigg). \tag{15}$$

The trilinear soft SUSY breaking parameters are, as usual in minimal GMSB, essentially zero at the scale of gauge mediation. The singlet S is a special case because it is a gauge singlet and, thus, would have a zero mass at this level. However, it gets a mass at the 3-loop level, which can be estimated to be

$$m_S^2 \simeq \frac{Y_S^2}{16\pi^2} (m_{\chi_R}^2 + m_{\nu^c}^2). \tag{16}$$

Obviously, this mass squared parameter is suppressed by an additional loop factor, and RGE effects usually drive it to negative values at the electroweak scale. However, as can be seen in Sec. III C 3, this is compensated by an F term proportional to $M_{Z'}^2$ yielding a positive mass squared for the corresponding mass eigenstates.

For completeness, we note that one can explain the neutrino data by adjusting μ_S and taking Y_ν as well as Y_S diagonal. μ_S is a small parameter, which does not affect the collider phenomenology. However, we will discuss in Sec. III E the effect of nondiagonal entries in Y_ν and Y_S in the range compatible with neutrino data on rare lepton decays.

D. Tadpole equations

We decompose the neutral scalar fields responsible for gauge symmetry breaking as usual:

$$H_u = \frac{1}{\sqrt{2}}(\sigma_u + i\phi_u + v_u), \quad H_d = \frac{1}{\sqrt{2}}(\sigma_d + i\phi_d + v_d),$$
$$\chi_R = \frac{1}{\sqrt{2}}(\sigma_R + i\phi_R + v_{\chi_R}), \quad \bar{\chi}_R = \frac{1}{\sqrt{2}}(\bar{\sigma}_R + i\bar{\phi}_R + v_{\bar{\chi}_R}). \tag{17}$$

We use the minimization conditions to determine the parameters $|\mu|^2$, $|\mu_R|^2$, B_μ, and B_{μ_R}:

$$B_\mu = \frac{t_\beta}{t_\beta^2 - 1} \Bigg(m_{H_d}^2 - m_{H_u}^2 + \frac{v^2}{4} c_{2\beta} (g_L^2 + g_Y^2 + (g_\chi - g_{Y\chi})^2) + \frac{5 v_R^2}{8} c_{2\beta_R} g_\chi (g_\chi - g_{Y\chi}) \Bigg), \tag{18}$$

$$B_{\mu_R} = \frac{t_{\beta_R}}{t_{\beta_R}^2 - 1}\Big(m_{\tilde{\chi}_R}^2 - m_{\chi_R}^2 - \frac{5v^2}{8} c_{2\beta} g_\chi (g_\chi - g_{Y_\chi}) + \frac{25 v_R^2}{16} c_{2\beta_R} g_\chi^2\Big), \tag{19}$$

$$|\mu|^2 = \frac{1}{t_\beta^2 - 1}\Big(m_{H_d}^2 - m_{H_u}^2 t_\beta^2 - \frac{v^2}{8}(g_L^2 + g_Y^2 + (g_\chi - g_{Y_\chi})^2)(t_\beta^2 - 1) + \frac{5 v_R^2}{16} c_{2\beta_R}(1 + t_\beta^2) g_\chi (g_\chi - g_{Y_\chi})\Big), \tag{20}$$

$$|\mu_R|^2 = \frac{1}{t_{\beta_R}^2 - 1}\Big(m_{\tilde{\chi}_R}^2 - m_{\chi_R}^2 t_{\beta_R}^2 + \frac{5v^2}{16} c_{2\beta}(t_{\beta_R}^2 + 1) g_\chi (g_\chi - g_{Y_\chi}) - \frac{25 v_R^2}{32}(t_{\beta_R}^2 - 1) g_\chi^2\Big), \tag{21}$$

where g_L is the $SU(2)_L$ gauge coupling, t_x, c_x, $s_x = \tan x$, $\cos x$, $\sin x$, whereas $\tan\beta = \frac{v_u}{v_d}$, $\tan\beta_R = \frac{v_{\chi_R}}{v_{\tilde{\chi}_R}}$, $v^2 = v_u^2 + v_d^2$, and $v_R^2 = v_{\chi_R}^2 + v_{\tilde{\chi}_R}^2$. Note, that the corresponding terms can be generated by the Giudice-Masiero mechanism [90] and are thus free parameters in our context.

The latter of these equations is of particular interest as it is responsible for one of the major limitations to the model. The 1-loop β functions for the soft-breaking masses read in the limit of vanishing kinetic mixing

$$\beta_{m_{\tilde{\chi}}^2}^{(1)} = -\frac{25}{2} g_\chi^2 |M_\chi|^2 + \frac{5}{2} g_\chi \sigma_\chi, \tag{22}$$

$$\beta_{m_{\tilde{\chi}}^2}^{(1)} = -\frac{25}{2} g_\chi^2 |M_\chi|^2 - \frac{5}{2} g_\chi \sigma_\chi + 2\,\mathrm{Tr}((m_\chi^2 + m_\nu^2) Y_S Y_S^\dagger + m_S^2 Y_S^\dagger Y_S + T_S^* T_S^T), \tag{23}$$

with

$$\sigma_\chi = \frac{g_\chi^2}{4}(5(m_{\tilde{\chi}_R}^2 - m_{\chi_R}^2) + 4(m_{H_d}^2 - m_{H_u}^2) + \mathrm{Tr}(m_{e^c}^2 + 3m_u^2 + 5m_{\nu^c}^2 + 6(m_Q^2 - m_L^2) - 9m_d^2)), \tag{24}$$

which is zero at the messenger scale and which stays zero if only 1-loop RGEs are used. One can see that the main differences in the running are stemming from terms that are proportional to the trilinear soft-breaking couplings or the soft-breaking masses. Since we will consider the minimal GMSB where nonvanishing trilinear couplings are only generated via RGE evolution and the breaking takes place well below the GUT scale, the splitting between the soft parameters $m_{\chi_R}^2$ and $m_{\tilde{\chi}_R}^2$ will, in general, be smaller in comparison to a scenario with gravity mediation. Because of Eq. (21), this immediately constrains $\tan\beta_R$ to be larger than but close to one. The terms proportional to the VEVs squared then only give negative contributions to $|\mu_R|^2$, i.e., there is an upper limit on $|v_R|$ depending on $\tan\beta_R$ to find a solution to the tadpole equations. In Fig. 1 we show $|\mu_R|$ in the v_R-$\tan\beta_R$ plane, in which one can see the correlation between the two parameters. Note that, in the upper white area, one cannot achieve the correct gauge symmetry breaking, whereas, in the lower white area, one encounters tachyonic states.

We have also considered the case where neutrino masses are generated by a seesaw type I mechanism similar to Ref. [77], in which case there is no need to introduce the singlet field $\hat{S}$. Technically, this amounts in replacing the terms $Y_S^{ij}\hat{\nu}_i^c \hat{S}_j \hat{\chi}_R + \mu_S^{ij}\hat{S}_i\hat{S}_j$ in Eq. (1) by $Y_S'^{ij}\hat{\nu}_i^c \hat{\chi}_R' \hat{\nu}_j^c$, where $\hat{\chi}_R'$ has twice the $U(1)$ charges of $\hat{\chi}_R$. Performing the same chain of calculations, one finds that there are hardly points with broken $U(1)_\chi$ as the larger gauge contributions in the RGE evolutions prevent $m_{\chi_R'}$ from becoming sufficiently small.

E. Higgs sector

In GMSB models with MSSM particle content, one needs a SUSY spectrum in the multi-TeV region to accommodate a Higgs mass of 125 GeV (see, e.g., Refs. [19,91,92]). The reason is that the trilinear soft SUSY breaking couplings are zero at the messenger scale in the minimal model, and thus the loop corrections to the Higgs boson masses get reduced. In our model, the additional $U(1)$ factor gives already a sizable D term contribution to the tree-level part of the Higgs mass, and thus the need for large loop corrections gets reduced.

On tree level, the scalar Higgs mass matrix in the basis $(\sigma_d, \sigma_u, \bar{\sigma}_R, \sigma_R)$ is given by

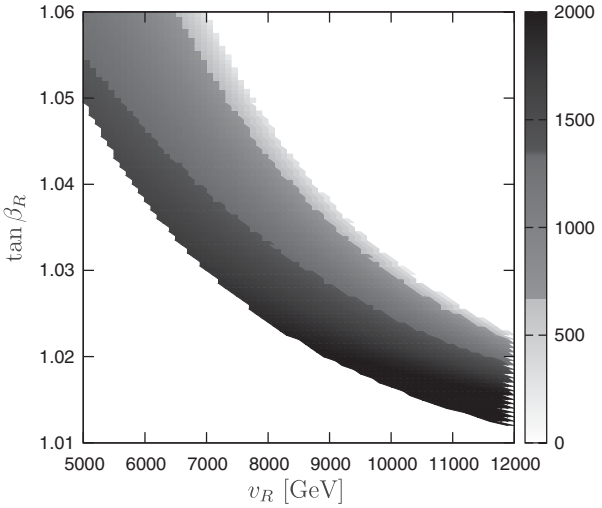

FIG. 1. Allowed parameter space in the $v_R - \tan\beta_R$ plane. The plotted values correspond to $|\mu_R|$, which is calculated using the tadpole equations. The free parameters have been set to $n = 1$, $\Lambda = 5\times10^5$ GeV, $M = 10^{11}$ GeV, $\tan\beta = 30$, $\mathrm{sign}(\mu_R) = -$, $\mathrm{diag}(Y_S) = (0.7, 0.6, 0.6)$, and $Y_\nu^{ii} = 0.01$.

$$m^2_{h^0} = \begin{pmatrix} \frac{1}{4}\tilde{g}^2_\Sigma v^2 c^2_\beta + m^2_A s^2_\beta & -\frac{s_{2\beta}}{8}(\tilde{g}^2_\Sigma v^2 + 4m^2_A) & \frac{5}{8}\tilde{g}^2_\chi v v_R c_\beta c_{\beta_R} & -\frac{5}{8}\tilde{g}^2_\chi v v_R c_\beta s_{\beta_R} \\ -\frac{s_{2\beta}}{8}(\tilde{g}^2_\Sigma v^2 + 4m^2_A) & \frac{1}{4}\tilde{g}^2_\Sigma v^2 s^2_\beta + m^2_A c^2_\beta & -\frac{5}{8}\tilde{g}^2_\chi v v_R s_\beta c_{\beta_R} & \frac{5}{8}\tilde{g}^2_\chi v v_R s_\beta s_{\beta_R} \\ \frac{5}{8}\tilde{g}^2_\chi v v_R c_\beta c_{\beta_R} & -\frac{5}{8}\tilde{g}^2_\chi v v_R s_\beta c_{\beta_R} & \frac{25}{16} g^2_\chi v^2_R c^2_{\beta_R} + m^2_{A_R} s^2_{\beta_R} & -\frac{s_{2\beta_R}}{32}(25 g^2_\chi v^2_R + 16 m^2_{A_R}) \\ -\frac{5}{8}\tilde{g}^2_\chi v v_R c_\beta s_{\beta_R} & \frac{5}{8}\tilde{g}^2_\chi v v_R s_\beta s_{\beta_R} & -\frac{s_{2\beta_R}}{32}(25 g^2_\chi v^2_R + 16 m^2_{A_R}) & \frac{25}{16} g^2_\chi v^2_R s^2_{\beta_R} + m^2_{A_R} c^2_{\beta_R} \end{pmatrix}, \quad (25)$$

where $\tilde{g}^2_\Sigma = g^2_L + g^2_Y + (g_\chi - g_{Y_\chi})^2$, $\tilde{g}^2_\chi = g_\chi(g_\chi - g_{Y_\chi})$, and s_x, $c_x = \sin x, \cos x$. The parameters m_A and m_{A_R} are the tree-level masses of the pseudoscalar Higgs bosons, which are given by $m^2_A = B_\mu/(s_\beta c_\beta)$ and $m^2_{A_R} = B_{\mu_R}/(s_{\beta_R} c_{\beta_R})$. Already at tree level, this leads to non-negligible contributions to the doublet Higgs mass as $\frac{1}{4}\tilde{g}^2_\Sigma v^2 \simeq M^2_Z + \frac{1}{4}v^2(g_\chi - g_{Y_\chi})^2 > M^2_Z$. As typical values, we find $g_\chi - g_{Y_\chi} \simeq 0.27$. This immediately gives an upper bound on the tree-level Higgs mass:

$$m_{h,\text{tree}} \leq M^2_Z + \frac{1}{4}(g_\chi - g_{Y_\chi})^2 v^2. \quad (26)$$

In Fig. 2, we show the dependence of the two lightest Higgs states on $\tan\beta_R$ at tree level. Even in this very restricted model, the tree-level mass can easily reach 100 GeV while at the same time requiring that this state is mainly an $SU(2)_L$ doublet Higgs boson. Even though the details are changed by loop corrections, see, e.g., Ref. [55], this figure also shows that $\tan\beta_R$ has to be close to 1 to obtain this desired feature. In the numerical part, we include the complete 1-loop correction to Eq. (25) and the dominant 2-loop corrections to the MSSM sub-block.

F. Dark matter

As already mentioned, the gravitino is the LSP in GMSB models, and all SUSY particles decay into it in a cosmologically short time [93–95]. The abundance of thermally produced gravitinos is under assumptions consistent with the standard thermal evolution of the early Universe given by

$$\Omega_{3/2}h^2 = \frac{m_{3/2}}{\text{keV}}\frac{100}{g_\star}. \quad (27)$$

Here, $g_\star$ is the effective number of degrees of freedom at the time of gravitino decoupling. For a mass of $O(100)$ eV, the gravitino would form warm dark matter and would have the correct abundance to explain the observed dark matter relic density in the Universe. However, there are stringent constraints on the contribution of warm dark matter from observations of the Lyman-α forest [96]. These bounds rule out pure warm dark matter scenarios with particle masses below 8 keV for nonresonantly produced dark matter [97]. If one takes this lower limit into account, one sees that gravitinos, which have once been in thermal equilibrium, would overclose the Universe. This is known as the cosmological gravitino problem. There have been some proposals in the literature to circumvent this problem by, for instance, additional entropy production after the freeze-out of the gravitino [98–100]. However, it turned out that entropy production from messenger decays hardly works [101]. Hence, one has to assume either other mechanisms like saxion decays [102] or decays of moduli fields [103]. Also, if the gravitino mass is in the MeV range, they might never have been in thermal equilibrium if the reheating temperature is sufficiently low [104]. Because of these very model dependent issues, we do not address the question of the gravitino relic density in the following.

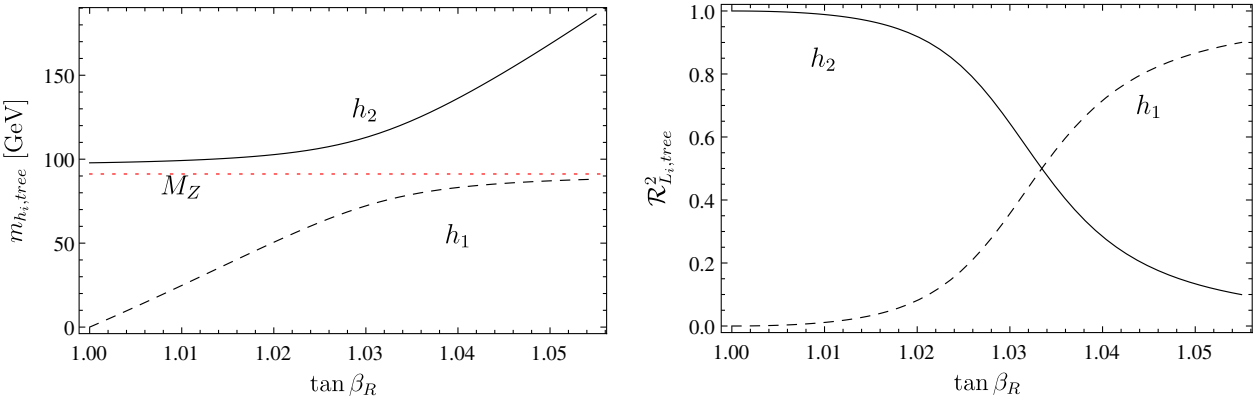

FIG. 2 (color online). Tree-level dependence of the lightest Higgs masses (left) as well as the admixture of the $SU(2)_L$ doublet Higgses $\mathcal{R}^2_{L_i} = |U_{i1}|^2 + |U_{i2}|^2$ (right) on $\tan\beta_R$ with the parameter choice of Fig. 1 and $v_R = 7$ TeV. The horizontal small dashed (red) line shows the Z mass.

III. NUMERICAL RESULTS

A. Implementation in SARAH and SPheno

We used the implementation of the model in SARAH [105–108] and SPheno [109,110] presented in Ref. [80] and extended it by the GMSB boundary conditions: here, we allow for up to four messenger **10**-plets with degenerated masses. At the messenger scale, we implemented the GMSB boundary conditions for the soft masses using the Eqs. (13)–(15). The link between SARAH and SPheno allows for a precise mass spectrum calculation based on full 2-loop RGE running and the 1-loop corrections to all masses. In addition, the known 2-loop corrections to the Higgs masses in the MSSM are linked [111–114]. For more details of the mass spectrum calculation as well as the inclusion of SUSY thresholds, we refer to Ref. [80]. In addition, the SPheno version created by SARAH includes also routines for a full 1-loop calculation of the LFV observables $l_i \to l_j\gamma$, $l_i \to 3l_j$, $\mu - e$ conversion in atoms, flavor violating τ decays to a lepton and meson, and $B_s \to \mu^+\mu^-$ [115].

For further discussions, we choose six benchmark scenarios BLRI–BLRVI, which provide distinct features. These benchmark points are given in Table III and will be discussed in the following Sec. III B.

B. Higgs physics

We performed a scan over the free parameter space in order to numerically check how well Higgs data can be accommodated for in our GMSB framework. The parameter variations can be found in Table IV. In Fig. 3, we show the masses of the doubletlike Higgs vs the mass of the lightest stop. As expected from the discussion in Sec. II E, points where h_2 is the doubletlike Higgs are of particular interest since they allow for higher values of the Higgs mass at a fixed $m_{\tilde{t}}$. Because of the tree-level contributions from the new sector, we can achieve the observed Higgs mass even for stop masses of about 2 TeV while a doubletlike h_1 requires $m_{\tilde{t}_1} \gtrsim 3$ TeV. Admittedly, this is quite a high scale in terms of naturalness in SUSY. However, compared to the lower limit of $m_{\tilde{t}} \gtrsim 5$ TeV, in usual GMSB scenarios (see, e.g., Ref. [91]), this is significantly

TABLE III. Input parameters and mass spectrum of different representative parameter points.

	BLRI	BLRII	BLRIII	BLRIV	BLRV	BLRVI
n		4		1	1	1
Λ [GeV]		2.5×10^5		5×10^5	3.8×10^5	5×10^5
M [GeV]		10^{11}		10^{10}	9×10^{11}	10^{11}
$\tan\beta$		40		30	30	20
$\tan\beta_R$		1.04		1.03	1.05	1.02
sign(μ_R)		$-$		$+$	$-$	$+$
v_R [TeV]		7		7.5	6.7	12
Y_ν^{ii}		0.01		0.01	0.01	0.01
diag(Y_S)	(0.65,0.65,0.1)	(0.65,0.65,0.3)	(0.65,0.65,0.65)	(0.6,0.6,0.6)	(0.77,0.73,0.45)	(0.7,0.6,0.6)
m_{h_1} [GeV]	70	92	125	70	108	98
$\mathcal{R}^2_{L,h_1}$	0.006	0.018	0.961	0.003	0.094	0.006
m_{h_2} [GeV]	126	127	156	124	124	124
$\mathcal{R}^2_{L,h_2}$	0.994	0.982	0.039	0.997	0.906	0.995
$M_{Z'}$ [TeV]		2.53		2.7	2.41	4.32
$m_{\nu_{h,1}}$ [GeV]	357	1070	2306	2277	1542	3633
$m_{\nu_{h,2}}$ [GeV]	2309	2308	2306	2278	2497	3633
$m_{\nu_{h,3}}$ [GeV]	2309	2308	2306	2278	2633	4238
$m_{\tilde{\nu}_1}$ [GeV]	334	909	1715	1728	1207	1863
$m_{\tilde{\nu}_2}$ [GeV]	1072	1546	1715	1757	1482	1879
$m_{\tilde{\nu}_3}$ [GeV]	2090	2048	1715	1759	1514	1879
$m_{\tilde{\tau}_1}$ [GeV]	906	906	905	867	764	1007
$m_{\tilde{\mu}_R}$ [GeV]	1166	1166	1165	976	877	1061
$m_{\tilde{e}_R}$ [GeV]	1167	1166	1166	976	877	1061
$m_{\tilde{\chi}_1^0}$ [GeV]	505	766	1156	575	453	589
$m_{\tilde{\chi}_2^0}$ [GeV]	1157	1157	1353	610	825	1043
$m_{\tilde{\chi}_1^\pm}$ [GeV]	2216	2216	2217	1113	883	1142
$m_{\tilde{\chi}_2^\pm}$ [GeV]	2591	2590	2588	1956	1600	2015
$m_{\tilde{g}}$ [GeV]	5460	5459	5456	3018	2423	3076
$m_{\tilde{t}_1}$ [GeV]	4209	4209	4206	2993	2231	2941

TABLE IV. Parameter ranges of the scan. The sign of μ has always been taken positive.

Parameter	Varied range
No. Messenger multiplets n	1...4
Messenger scale M	$(10^5 \ldots 10^{12})$ GeV
$\Lambda = F/M$	$\frac{1}{\sqrt{n}}(10^5 \ldots 10^6)$ GeV
$\tan\beta$	1.5...40
$\tan\beta_R$	1...1.15
$\mathrm{sign}(\mu_R)$	± 1
v_R	(6.5 ... 10) TeV
Y_S^{ii}	0.01...0.8
Y_ν^{ii}	$10^{-5} \ldots 0.5$

lower. Such a heavy stop will be difficult to study at the LHC and will potentially require a center of mass (c.m.) energy larger than 14 TeV. However, here, an e^+e^- collider like CLIC with up to 5 TeV c.m. energy might be an ideal machine to discover and study such a heavy stop; see, e.g., Refs. [116,117] and references therein.

A way to allow for a lighter SUSY spectrum in GMSB scenarios apart from the mixing with the extended Higgs sector is going up to higher messenger scales, thus allowing a longer RGE running and hence larger induced T parameters as demonstrated in Fig. 4. At $M \simeq 10^{10}$ and 10^{11} GeV, there is a level crossing between the two light states for the points BLRIII and BLRV, respectively, which is the reason for the observed increase of m_h.

An interesting observable is the rate $h \to \gamma\gamma$ as there are some hints for an enhancement above SM expectations [118–120]. We define the ratio $R_{h\to\gamma\gamma}$ by

$$R_{h\to\gamma\gamma} = \frac{[\sigma(pp \to h) \times \mathrm{BR}(h \to \gamma\gamma)]_{\mathrm{BLR}}}{[\sigma(pp \to h) \times \mathrm{BR}(h \to \gamma\gamma)]_{\mathrm{SM}}}. \quad (28)$$

The cross sections for the main production channels, gluon fusion, and vector boson fusion are essentially the SM-production cross section reweighted by the (effective) couplings of the Higgs boson c_{hXX}^{BLR} normalized to the SM expectations c_{hXX}^{SM}:

$$\sigma(XX \to h)_{\mathrm{BLR}} = \sigma(XX \to h)_{\mathrm{SM}} \left(\frac{c_{hXX}^{\mathrm{BLR}}}{c_{hXX}^{\mathrm{SM}}}\right)^2, \qquad X = g, W. \quad (29)$$

The main contribution to Higgs production comes from gluon fusion. The effective Higgs coupling to two gluons is completely determined in the SM by the top and W loop.

In supersymmetric models, an enhancement can be achieved via a light stau. In models with extended gauge structures, such a light stau and thus an enhancement of the $\gamma\gamma$ rate can be obtained even in scenarios with large soft SUSY breaking parameters [121], as there are large negative contributions due to the D terms of the extra $U(1)$ to the stau mass. However, in the model considered here, this does not work for two reasons: the large stop mass required to obtain the correct Higgs mass implies a lower limit on Λ, and, secondly, the D term itself is smaller in our model compared to the one of Ref. [121] taking the same Z' mass and ratio of additional VEVs as demonstrated in Fig. 5. In this restricted model, the tadpole equations imply that a larger v_R requires a smaller $\tan\beta_R$, and thus the D terms cannot be enhanced to the required level. In Fig. 6, we show $R_{h\to\gamma\gamma}$ as a function of the stau mass, demanding that the mass of the doubletlike Higgs be in the range $123\ \mathrm{GeV} < m_h < 128\ \mathrm{GeV}$. This implies a lower limit on $m_{\tilde{\tau}_1} \gtrsim 500$ GeV, which is too large to get a sizable contribution to $h \to \gamma\gamma$, and thus we find $R_{h\to\gamma\gamma} \lesssim 1$ in this model. Hence, this model will be excluded if $R_{h\to\gamma\gamma} > 1$ is established by ATLAS and CMS at a significant level. However, the most recent results of CMS point exactly in this direction that the diphoton rate is in good agreement with SM expectations [122].

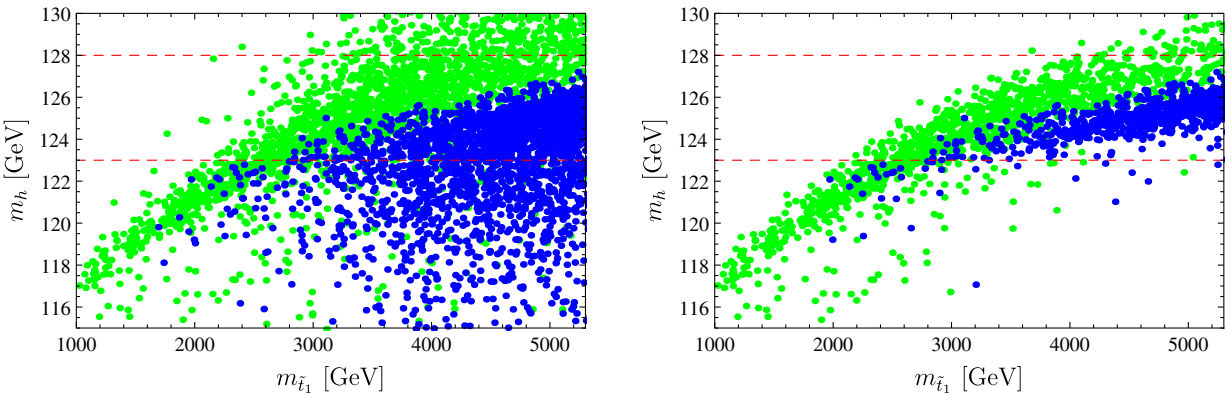

FIG. 3 (color online). Mass of the doublet-like Higgs vs the mass of the lightest stop for $n = 1$ and the other parameters as in Table IV. Only points with $R_{h\to\gamma\gamma} > 0.5$ (left) and 0.9 (right) were included. The blue dots represent points where the lightest eigenstate is doublet-like, green dots where it is the second-lightest Higgs.

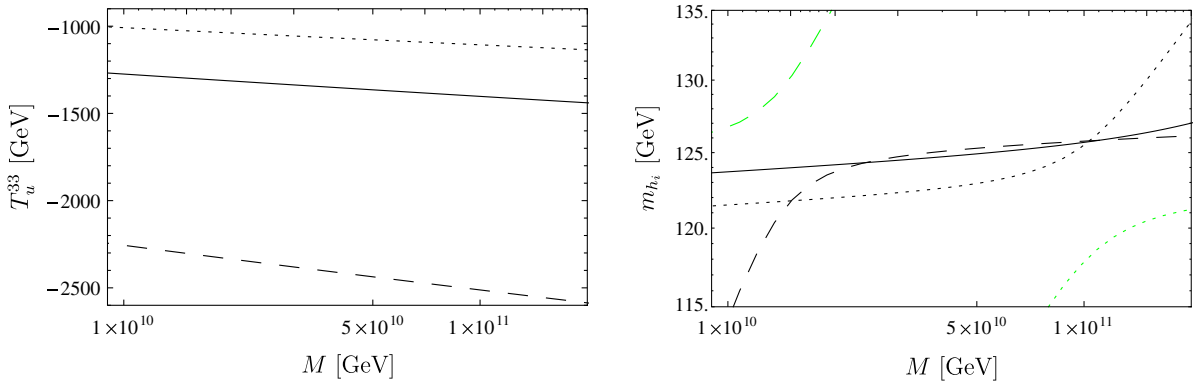

FIG. 4 (color online). T_u^{33} and mass of the doubletlike Higgs vs M for BLRIII (black dashed line), BLRIV (black full line), and BLRV (black dotted line) (but for $\tan\beta_R = 1.03$). The light green lines correspond to the χ_R-like Higgs state of the corresponding parameter point.

C. Next-to-lightest SUSY particle

As usual in GMSB models, the gravitino $\tilde{G}$ is the LSP, and its mass is given by [87]

$$m_{3/2} = \frac{F}{\sqrt{3} m_{\mathrm{Pl}}}, \tag{30}$$

with the reduced Planck mass m_{Pl}. The gravitino mass is usually in the MeV range or above due to large messenger scales required to obtain the correct symmetry breaking. In our model are three possibilities for the next-to lightest supersymmetric particle (NLSP): the two usual candidates, which are the lightest neutralino and the lightest slepton, which is usually a stau, and, in addition, our model contains the lightest sneutrino as the third candidate. In general, we can state that the lightest neutralino will be the NLSP for low messenger multiplicities, $n \lesssim 2$, and little hierarchy in the diagonal entries of Y_S. For larger n, $\tilde{\chi}_1^0$ can only be lighter than the lightest slepton if the left-right-splitting of the stau is small (i.e., for low $\tan\beta$ values) or if $|\mu_R|$ is small. We discuss the different character of a neutralino NLSP in the next Sec. III C 1. Otherwise, i.e., for large n and nonhierarchical Y_S, the stau is the NLSP. A sneutrino can be the NLSP for all n if there is a large hierarchy in the Y_S entries: the scalar singlet field corresponding to the smallest Y_S entry gets light. In the following, we present the corresponding mass matrices and discuss briefly the main differences compared to the phenomenology of the usual minimal GMSB model using the parameter points in Table III. As the lifetime of the NLSP is proportional to F^2 [87], we find that, in most of the available parameter space, the NLSP is so long-lived that it will leave a typical collider detector before decaying. However, its lifetime is, in general, still below the bounds set by big bang nucleosynthesis.

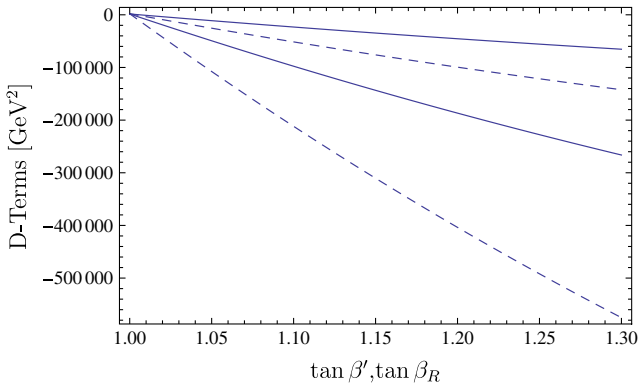

FIG. 5 (color online). D term contribution to the mass entries of the R sleptons for $\tan\beta = 10$, $M_{Z'} = 1.5$, 3.0 TeV, and fixing the gauge couplings by the requirement of gauge coupling unification: $g_{BL}^{Y\times BL} = 0.55$, $g_Y = 0.36$, respectively, $g_{BL}^{R\times B-L} = 0.57$, $g_R = 0.45$. The full (dashed) lines correspond to the $U(1)_R \times U(1)_{B-L}$ ($U(1)_Y \times U(1)_{B-L}$) scenario.

1. Neutralinos

This model contains seven neutralinos, which are, besides the usual MSSM gauginos and Higgsinos, the extra $U(1)$ gaugino λ_χ and the two R Higgsinos $\tilde{\chi}_R$ and $\tilde{\tilde{\chi}}_R$. In the basis $(\lambda_Y, \lambda_{W^3}, \tilde{h}_d^0, \tilde{h}_u^0, \lambda_\chi, \tilde{\tilde{\chi}}_R, \tilde{\chi}_R)$, the mass matrix reads

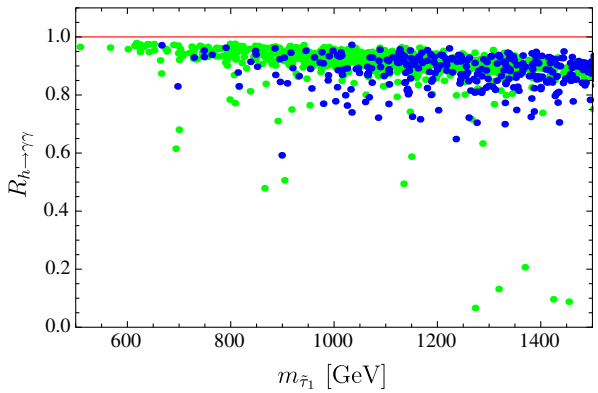

FIG. 6 (color online). Decay rate of $h \to \gamma\gamma$ as a function of the stau mass using four **10**-plets. Only points with 123 GeV $< m_h <$ 128 GeV are included. Color coding of the parameter points is as in Fig. 3.

$$M_{\tilde{\chi}^0} = \begin{pmatrix} M_1 & 0 & -\frac{g_Y v_d}{2} & \frac{g_Y v_u}{2} & \frac{M_{Y_\chi}}{2} & 0 & 0 \\ 0 & M_2 & \frac{g_L v_d}{2} & -\frac{g_L v_u}{2} & 0 & 0 & 0 \\ -\frac{g_Y v_d}{2} & \frac{g_L v_d}{2} & 0 & -\mu & \frac{(g_\chi - g_{Y_\chi}) v_d}{2} & 0 & 0 \\ \frac{g_Y v_u}{2} & -\frac{g_L v_u}{2} & -\mu & 0 & -\frac{(g_\chi - g_{Y_\chi}) v_u}{2} & 0 & 0 \\ \frac{M_{Y_\chi}}{2} & 0 & \frac{(g_\chi - g_{Y_\chi}) v_d}{2} & -\frac{(g_\chi - g_{Y_\chi}) v_u}{2} & M_\chi & \frac{5 g_\chi v_{\chi_R}}{4} & -\frac{5 g_\chi v_{\chi_R}}{4} \\ 0 & 0 & 0 & 0 & \frac{5 g_\chi v_{\chi_R}}{4} & 0 & -\mu_R \\ 0 & 0 & 0 & 0 & -\frac{5 g_\chi v_{\chi_R}}{4} & -\mu_R & 0 \end{pmatrix}. \quad (31)$$

For a first understanding, it is useful to neglect the mixing between the MSSM states and the additional ones. In this case, one gets $M^2_{Z'} \simeq \frac{25}{16} g^2_\chi v^2_R$, and, in the limit $\tan\beta_R \to 1$, one finds for the eigenvalues of the three additional neutralino states

$$\mu_R, \frac{1}{2}\left(M_\chi + \mu_R \pm \sqrt{\frac{1}{4} M^2_{Z'} + M^2_\chi - 2 M_\chi \mu_R + \mu^2_R} \right). \quad (32)$$

In most of the parameter space, one finds $|\mu_R|, M_\chi \ll M_{Z'}$, and thus one has one state with mass $|\mu_R|$ and two states with masses close to $M_{Z'}$, which can even form a quasi-Dirac state. For the MSSM-like states, the lightest one is always binolike, and thus we find, depending on the ratio $|\mu_R|/M_1$, that the lightest neutralino is either binolike or a nearly maximal mixed $\tilde{\chi}_R - \tilde{\chi}_R$ state. This is exemplified in Fig. 7 for the point BLRIV with a slight adjustment of $\tan\beta_R$ to satisfy the tadpole equation (21). Here, the NLSP nature changes from $\tilde{\chi}_R$-like to binolike at about $\mu_R \simeq 575$ GeV.

The lightest neutralino will decay dominantly into a χ_R-like Higgs state and a gravitino $\tilde{G}$ if it is mainly a $\tilde{\chi}_R$ Higgsino, whereas the MSSM-like bino state decays dominantly into $\gamma\tilde{G}$ and $Z\tilde{G}$ as depicted in Fig. 8. However, as

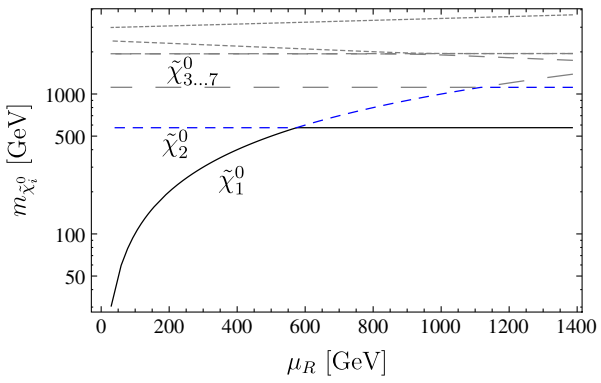

FIG. 7 (color online). Neutralino masses as a function of μ_R for the point BLRIV ($M_1 \simeq 575$ GeV) and $1.02 \leq \tan\beta_R \leq 1.033$ to satisfy the tadpole equation (21).

mentioned above, the neutralinos are rather long-lived, and thus, at the LHC, they will decay, in general, outside the detectors. Hence, new techniques would be necessary to observe these states. For $|\mu_R| < M_1$, we find that h_{χ_R} can be produced in the decays of $\tilde{\chi}^0_2$ at a sizable rate. Therefore, SUSY cascade decays offer the possibility to study this particle, which can hardly be produced directly or in Higgs decays.

The large values of Λ imply that the squarks and the gluino are usually in the multi-TeV range, implying that one will need the high luminosity option of the LHC to study these particles in detail. It turns out that the two lightest states are $\tilde{g}$ and $\tilde{t}_1$. Depending on $m_{\tilde{g}} - m_{\tilde{t}_1}$, the gluino decays either dominantly into third-generation quarks and neutralinos/charginos or into $t\tilde{t}_1$. In both cases, the final states will contain b jets and W bosons. Depending on the nature of the two lightest neutralinos, also a Higgs boson can be in the final state as discussed above. Moreover, also, the additional sneutrinos can appear in the cascade decays, but distinguishing them from the usual MSSM sneutrinos will be rather difficult.

2. Charged sleptons

The mass matrix of the sleptons reads in the basis $(\tilde{e}_L, \tilde{e}_R)$

$$m^2_{\tilde{l}} = \begin{pmatrix} m^2_L + \frac{1}{2} v^2 c^2_\beta Y^\dagger_e Y_e + D_L \mathbf{1} & \frac{v}{\sqrt{2}}(T^\dagger_e c_\beta - \mu Y^\dagger_e s_\beta) \\ \frac{v}{\sqrt{2}}(T_e c_\beta - \mu^* Y_e s_\beta) & m^2_E + \frac{1}{2} v^2 c^2_\beta Y_e Y^\dagger_e + D_R \mathbf{1} \end{pmatrix}, \quad (33)$$

which has the same structure as in the MSSM, but, for the concrete form of the D terms,

$$D_L = \frac{1}{32}(2(-3g^2_\chi + g_\chi g_{Y_\chi} + 2(g^2_Y - g^2_L + g^2_{Y_\chi}))v^2 c_{2\beta} - 5 g_\chi (3 g_\chi + 2 g_{Y_\chi}) v^2_R c_{2\beta_R}), \quad (34)$$

$$D_R = \frac{1}{32}(2(g^2_\chi + 3 g_\chi g_{Y_\chi} - 4(g^2_Y + g^2_{Y_\chi}))v^2 c_{2\beta} + 5 g_\chi (g_\chi + 4 g_{Y_\chi}) v^2_R c_{2\beta_R}). \quad (35)$$

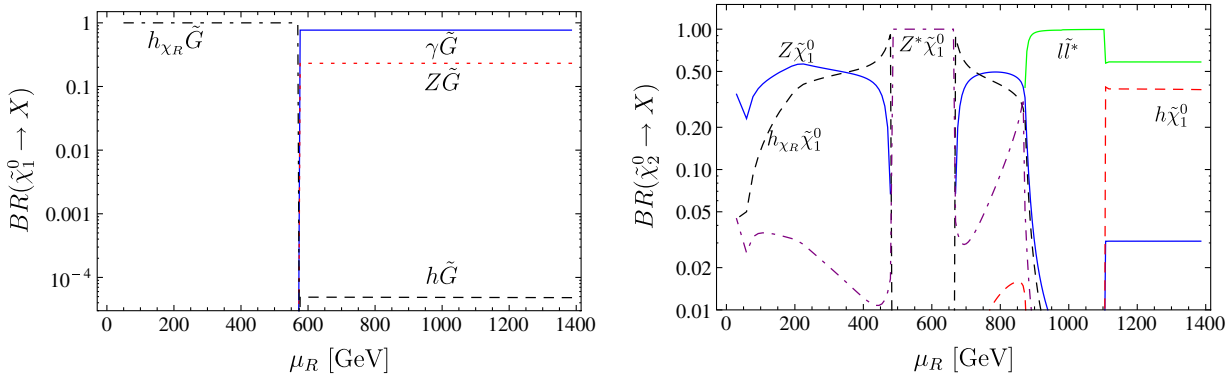

FIG. 8 (color online). Branching ratios of $\tilde{\chi}_1^0$ (left) and of $\tilde{\chi}_2^0$ (right) as a function of μ_R for the same parameter choice as in Fig. 7.

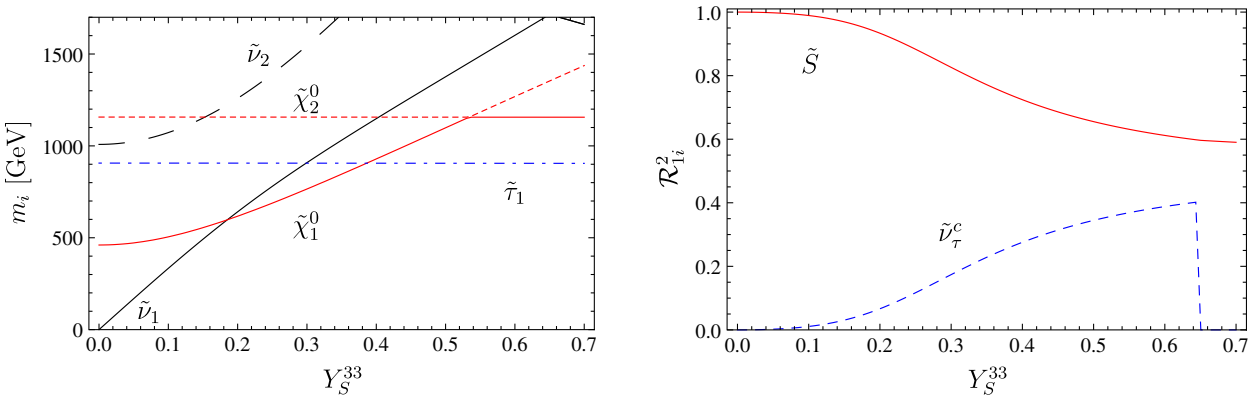

FIG. 9 (color online). Masses of the lightest SUSY particles (left) and the sneutrino composition (right) as a function of Y_S^{33} for the parameters specifying the points BLRI, BLRII, and BLRIII. In the right plot, the full red (dashed blue) line gives the $\tilde{S}$ ($\tilde{\nu}_\tau^c$) contribution to the nature of the lighest sneutrino.

As explained above, stau NLSPs can be obtained for $n \geq 3$ and large values of $\tan\beta$ as left-right mixing can compensate the additional D terms. As can be seen in Fig. 9, the three diagonal entries of Y_S have to be of roughly the same size.

As indicated in Table III, the gluino is usually very heavy, and it turns out that it is the heaviest strongly interacting particle. This implies that one will need a very high luminosity to discover this particle. In general, it decays into all squarks, which in turn decay further into the MSSM-like neutralinos and charginos. Note, that both light Higgs states, the doubletlike one as well as the h_{χ_R}-like one, can be produced in these decays. Finally, the lightest neutralino will decay into $\tau\tilde{\tau}_1$, and $\tilde{\tau}$ will, in general, decay outside the detector. Thus, a typical event will consist of several jets and leptons plus a charged track from a (at the detector level) stable particle. The phenomenology of long-lived staus has already been studied comprehensively in the literature; see, e.g., Refs. [123,124], and bounds of $m_{\tilde{\tau}} \gtrsim 300$ GeV have been set by the LHC collaborations [125] in MSSM scenarios.

3. Sneutrinos

As it is well-known, in inverse seesaw scenarios, the parameter μ_S has to be small to explain correctly neutrino data.[1] For completeness, we note that the inverse seesaw mechanism yields in this model three very light Majorana states, which can explain the observed neutrino data where the six heavier neutrinos are pairwise degenerate forming three quasi-Dirac states [80]. We will denote the former by ν and the latter by ν_h. The F terms induced by μ_S as well as the corresponding soft SUSY breaking term $B_{\mu_S}\tilde{S}\,\tilde{S}$ induce a splitting of the complex sneutrino fields into their scalar and pseudoscalar components. However, in practice, this mass splitting is tiny, and thus we can safely neglect it in the following discussion. In the limit $\mu_S, B_{\mu_S} \to 0$, the sneutrino mass matrix reads in the basis $(\tilde{\nu}, \tilde{\nu}^c, \tilde{S})$

[1]For a discussion and the corresponding mass matrix, see, for example, Ref. [80] and references therein.

$$M^2_{\tilde{\nu}} = \begin{pmatrix} m_L^2 + \frac{v^2 s_\beta^2}{2} Y_\nu^\dagger Y_\nu + D'_L \mathbf{1} & \frac{v}{\sqrt{2}}(T_\nu^\dagger s_\beta - \mu Y_\nu^\dagger c_\beta) & \frac{1}{2} v v_R Y_\nu^\dagger Y_S s_\beta s_{\beta_R} \\ \frac{v}{\sqrt{2}}(T_\nu s_\beta - \mu^* Y_\nu c_\beta) & m^2_{\nu^c} + \frac{v_R^2 s^2_{\beta_R}}{2} Y_S Y_S^\dagger + \frac{v^2 s_\beta^2}{2} Y_\nu Y_\nu^\dagger + D'_R \mathbf{1} & \frac{v_R}{\sqrt{2}}(T_S s_{\beta_R} - \mu_R^* Y_S c_{\beta_R}) \\ \frac{1}{2} v v_R Y_S^\dagger Y_\nu s_\beta s_{\beta_R} & \frac{v_R}{\sqrt{2}}(T_S^\dagger s_{\beta_R} - \mu_R Y_S^\dagger c_{\beta_R}) & m_S^2 + \frac{v_R^2 s^2_{\beta_R}}{2} Y_S^\dagger Y_S \end{pmatrix}, \quad (36)$$

with

$$D'_L = \frac{1}{32}(2(-3g_\chi^2 + g_\chi g_{Y_\chi} + 2(g_L^2 + g_Y^2 + g_{Y_\chi}^2))v^2 c_{2\beta} - 5g_\chi(3g_\chi + 2g_{Y_\chi})v_R^2 c_{2\beta_R}), \quad (37)$$

$$D'_R = \frac{5g_\chi}{32}(2(g_\chi - g_{Y_\chi})v^2 c_{2\beta} + 5g_\chi v_R^2 c_{2\beta_R}). \quad (38)$$

Obviously, the masses of the sneutrinos depend strongly on Y_S. In particular, $\tilde{S}$-$\tilde{S}$ entries are dominated by $\frac{v_R^2 s^2_{\beta_R}}{2} Y_S^\dagger Y_S$ because m_S^2 is rather small, as discussed in Sec. II C. Therefore, even $m_S^2 < 0$ does not automatically imply spontaneous R parity breaking. The $\tilde{\nu}^c$-$\tilde{S}$ mixing entry can be of the same size as the corresponding diagonal entries for sufficiently large $|\mu_R|$. The entries which mix these states with $\tilde{\nu}_L$ are much smaller and can be neglected for the moment. As $\tan\beta_R$ is close to 1, we can take the limits $\tan\beta_R \to 1$, $D'_R \to 0$ and find for these approximations the upper bound,

$$|\mu_R| \lesssim \sqrt{m^2_{\nu^c} + v_R^2 Y_S^2/4}, \quad (39)$$

to avoid tachyonic states. Here, we have also set $T_S = 0$, as this is numerically always small. For completeness, we note that $|Y_S Y_S^\dagger|$ is bounded from above by the requirement that all couplings stay perturbative up to the GUT scale and from below by the requirement of correct symmetry breaking as discussed in Sec. II D.

Combining all requirements, we find a light sneutrino, which could be the NLSP, if one of the diagonal Y_S entries is rather small, $\lesssim 0.2$, and the other two are large, ~ 0.7. In an abuse of language, we call this state a sneutrino, even though the corresponding state is dominantly a $\tilde{S}$. However, it still can have a sizable $\tilde{\nu}^c$ admixture as exemplified in Fig. 9. Note that taking Y_S^{33} small is an arbitrary choice, and we could have equally well taken one of the two other generations. The smallness of this coupling also implies that one of the heavy quasi-Dirac neutrinos is significantly lighter than the other two, but we find that this state is always heavier than the lightest sneutrino. Therefore, a sneutrino NLSP decays always invisibly into $\nu\tilde{G}$. As can be seen in Fig. 9, the next heavier state is $\tilde{\chi}_1^0$, which turns out to be mainly a $\tilde{\chi}_R$ Higgsino. If kinematically allowed, it will decay to $\tilde{\nu}_1 \nu_h$, yielding

$$\tilde{\chi}_1^0 \to \tilde{\nu}_1 \nu_h \to \nu \tilde{G} W^{(*)} l, \quad (40)$$

giving a final state with an (off-shell) W boson, the lepton of the corresponding generation and missing energy. For completeness, we note that we find $\mathrm{BR}(\tilde{\chi}_1^0 \to \tilde{\nu}_1 \nu_h) \simeq 1$ if $|Y_S^{33}| \lesssim 0.07$ for the parameters used in Fig. 9 and $\mathrm{BR}(\tilde{\chi}_1^0 \to \tilde{\nu}_1 \nu) \simeq 1$ for larger values of $|Y_S^{33}|$. The latter leads to a completely invisible final state, and thus, in this part of the parameter space, this scenario cannot be distinguished from the $\tilde{\chi}_1^0$ NLSP case in this model.

D. Z' phenomenology

The LHC collaborations ATLAS and CMS have recently updated the bounds on $M_{Z'}$ from the search for dilepton resonances [126,127] at $\sqrt{s} = 8$ TeV and an integrated luminosity of about 20 fb^{-1} each. In order to apply these bounds to our model, we calculate the production cross section of the Z' and the subsequent decay into a pair of leptons as a function of the Z' mass.[2] From Fig. 10, one can extract the limits that depend on the underlying parameters. In case of BLRIII (dashed line), only standard model decay channels for the Z' are open, leading to a bound of about 2.43 TeV, whereas it can be reduced to about 2.37 TeV if, in addition, decays into heavy neutrinos and sneutrinos are allowed as is the case of BLRI (full line). This translates into a lower limit on v_R of about $v_R \gtrsim 6.6$ TeV.

As already mentioned, the colored SUSY particles are rather heavy in this model in most of the parameter space once the constraint on the Higgs mass is imposed implying that the discovery of supersymmetry requires either a huge statistics and/or a larger c.m. energy. However, it has been shown that the decays of the Z' open the possibility to produce SUSY particles [76,80,130–134]. As has been discussed in Ref. [80] in a constrained-MSSM–like variant of this model, the potentially interesting final states from Z' decays are: $\nu_h \nu_h$, $\tilde{l}\tilde{l}$, $\tilde{\nu}\tilde{\nu}$, $\tilde{\chi}_i^+ \tilde{\chi}_i^-$, and $\tilde{\chi}_i^0 \tilde{\chi}_j^0$. However, it turns out that, in the GMSB variant, the required conditions for the different channels are harder to realize, as this model is more constrained. In particular, we hardly find charged sleptons except for the case that $M_{Z'}$ is above 4 TeV because it couples significantly stronger to L sleptons than to R sleptons. In Table V, we list the Z' decay modes of the parameter points given in Table III.

The most important nonstandard decays of Z' are those into heavy neutrinos. Their masses are proportional to

[2]We used CalcHEP 3.4.2 [128] for the cross section calculation. The model was implemented using the SUSY Toolbox [129].

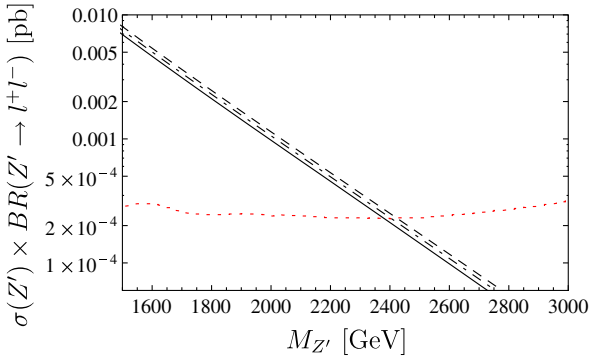

FIG. 10 (color online). $\sigma(pp \to Z' \to l^+l^-)$ as a function of $M_{Z'}$ for the scenarios BLRI (solid line), BLRII (dotted-dashed line), and BLRIII (dashed line). The red dotted line shows the exclusion limits at 95% C.L. obtained by ATLAS [126].

$\sqrt{Y_\nu^2 + Y_S^2}v_R$, implying that the corresponding Yukawas should not be too large because otherwise these decays are kinematically forbidden. This can clearly be seen by combining Tables III and V: the smaller the Y_S, the larger the corresponding branching is (for fixed Y_ν). The heavy neutrinos decay into Wl, $Z\nu$, and $h\nu$ with a branching ratio of ~0.6, ~0.2, and ~0.2, respectively [80]. Here, h denotes the doubletlike Higgs boson.

Naively, one would expect that also sneutrinos should show up in such scenarios because, as discussed in Sec. III C 3, the smaller the Y_S, the smaller the mass of the lightest sneutrino. However, at the same time, the $\tilde{S}$ component increases, as can be seen in Fig. 9, which reduces the coupling to the Z'. For an intermediate range of Y_S, the second lightest sneutrino can be produced in Z' decays. It decays dominantly according to

$$\tilde{\nu}_2 \to \nu_h \tilde{\chi}_1^0 \to \nu_h \nu_h \tilde{\nu}_1 \to llWW + \not{E}_T, \tag{41}$$

yielding

TABLE V. Branching ratios of the Z' boson for the parameter points of Table III. Only branching ratios larger than 10^{-2} are shown.

	BLRI	BLRII	BLRIII	BLRIV	BLRV	BLRVI
$M_{Z'}$ [TeV]		2.5		2.7	2.4	4.3
BR($d\bar{d}$)	0.45	0.49	0.52	0.52	0.52	0.48
BR($u\bar{u}$)	0.08	0.09	0.10	0.10	0.10	0.09
BR($l\bar{l}$)	0.17	0.18	0.20	0.20	0.20	0.18
BR($\nu\nu$)	0.15	0.16	0.17	0.17	0.17	0.16
BR(W^+W^-)	0.01	0.01	0.01	0.01	0.01	0.01
BR($\nu_h\nu_h$)	0.12	0.06	...	...	...	...
BR(h_1Z)	...	...	0.01	...	...	...
BR(h_2Z)	...	...	...	0.01	...	...
BR($\tilde{l}\tilde{l}^*$)	...	...	...	...	...	0.02
BR($\tilde{\nu}\,\tilde{\nu}$)	0.01	...	...	...	...	0.01
BR($\tilde{\chi}_i^0\tilde{\chi}_j^0$)	...	...	...	...	...	0.02
BR($\tilde{\chi}_2^+\tilde{\chi}_2^-$)	...	...	...	...	...	0.02

$$Z' \to \tilde{\nu}_2\tilde{\nu}_2^* \to 4l4W\not{E}_T \tag{42}$$

as a final state. The other final states are $2l2W2Z\not{E}_T$, $2l2W2h\not{E}_T$, $4Z\not{E}_T$, $2Z2h\not{E}_T$, and $4h\not{E}_T$, where h denotes again the doubletlike Higgs boson. We note for completeness that, for some part of the parameter space, also the decay $\tilde{\nu}_2 \to \tilde{\nu}_1 h_{\chi_R}$ is possible offering, in principle, a possiblity to observe h_{χ_R}. As $\tilde{\nu}_2$ is relatively heavy, there is a kinematical suppression, and we find only branching ratios of at most $O(0.01)$ for sneutrinos in the final state.

The Z' couples to all Higgsino states and the corresponding coupling is proportional to

$$g_\chi(2(Z_\chi^{i,3}Z_\chi^{j,3} - Z_\chi^{i,4}Z_\chi^{j,4}) + 5(Z_\chi^{i,6}Z_\chi^{j,6} - Z_\chi^{i,7}Z_\chi^{j,7})). \tag{43}$$

Here, Z_χ is the unitary matrix, which diagonalizes the neutralino mass matrix. As discussed above, the $\tilde{\chi}_R$-like neutralinos can be rather light. However, its admixture is such that $Z_\chi^{1,6} \simeq Z_\chi^{1,7} \simeq \pm 1/\sqrt{2}$, and thus this final state has only a tiny branching ratio. For large $M_{Z'}$, the decays into to the heavy MSSM charginos/neutralinos containing a sizable Higgsino component are kinematically allowed with a branching ratio of a few percent, as can be seen in Table V. In this scenario, the production cross section for the Z' is about 1 fb, and thus again large statistics are needed to observe and study the corresponding final states.

E. Lepton flavor violation

So far, we have assumed that neutrino mixing is explained by the flavor struture of μ_S, which hardly plays a role for the phenomenology discussed so far. In this case, also the rates for flavor violating lepton decays are very small and cannot be observed in the near future. However, as can be seen from the seesaw approximation of the neutrino mass matrix [135],

$$m_\nu^{IS} \simeq \frac{v_u^2}{v_R^2} Y_\nu^T Y_S^{-1} \mu_S (Y_S^T)^{-1} Y_\nu, \tag{44}$$

neutrino mixing can also be explained by the flavor structure of Y_ν and Y_S. As one can always find a basis where Y_S is diagonal on the expense of having nondiagonal Y_ν and μ_S, we will now consider the other extreme case in which the complete flavor structure resides in Y_ν. Nondiagonal Y_ν induces also nondiagonal entries in the soft-breaking terms of sleptons. However, as the scale for the GMSB boundary is lower than the GUT scale, the corresponding effects are significantly smaller compared to typical SUGRA scenarios. Therefore, the main effect is due to the vertices for which the off-diagonal entries of Y_ν enter. To study the corresponding effects in our model, we parametrize Y_ν according to [61]:

$$Y_\nu = f\begin{pmatrix} 0 & 0 & 0 \\ a & a\left(1-\frac{\sin\theta_{13}}{\sqrt{2}}\right) & -a\left(1+\frac{\sin\theta_{13}}{\sqrt{2}}\right) \\ \sqrt{2}\sin\theta_{13} & 1 & 1 \end{pmatrix},$$
$$a = \left(\frac{\Delta m^2_\odot}{\Delta m^2_{\rm Atm}}\right)^{\frac{1}{4}} \approx 0.4, \quad (45)$$

using the latest data from the global fit of the PMNS matrix [136]. This fixes Y_ν up to a global free prefactor f, which determines the rate for flavor violating decays like $\mu \to e\gamma$ or $\mu \to 3e$. Their branching ratios are constrained by experiment to be smaller than 5.7×10^{-13} and 10^{-12}, respectively [137,138]. In addition, the μ-e conversion rate (CR) in gold turns out to be important, which has to be smaller than 7×10^{-13} [139].

In Fig. 11, we show these rates as a function of f for the two points BLRI and BLRIII. We observe that, in these scenarios, $CR(\mu - e, \text{Au})$ is the most constraining observable followed by $\text{BR}(\mu \to 3e)$ and/or $\text{BR}(\mu \to e\gamma)$. As explained in detail in Refs. [140–142], this behavior can be understood as a nondecoupling effect of the Z-boson contribution to $CR(\mu - e, \text{Au})$ and $\text{BR}(\mu \to 3e)$, which are enhanced by a factor $(m_{\rm SUSY}/M_Z)^4$ with respect to the off-shell photon contributions, which is sizable due to the required heavy SUSY spectrum. In all cases, the sneutrino-chargino loops give the dominant contributions. We find that $CR(\mu - e, \text{Au})$ gives the strongest constraint on the size of f for all points of Table III. For completeness, we note that, once the bounds on this observable are fulfilled, we find that the corresponding LFV decays of the τ are so suppressed that they are below the reach of experiments in the near future. This implies, on the other hand, that, if, for example, one of the LHC experiments observes, for example, $\tau \to 3\mu$, then this class of models is ruled out.

A point worth mentioning here is a rather strong dependence of $\text{BR}(\mu \to e\gamma)$ on the sign of μ_R, which can change the rate by 1 order of magnitude. The reason is that the off-diagonal elements for the $\tilde{\nu}^c$-$\tilde{S}$ mixing in Eq. (37) are dominated by the $\mu_R \upsilon_R$ contribution as discussed in Sec. III C 3. We exemplify this behavior in Fig. 12, where we show $\text{BR}(\mu \to e\gamma)$ as a function of M for both signs of μ_R, $f = 0.03$ and fix the other parameters as for BLRIV. The black lines give all contributions, whereas, for the light green lines, we have taken out the contributions containing the Higgsino-like chargino. As a consequence, $\text{BR}(\mu \to e\gamma)$ could be in the reach of an upgraded version of the MEG experiments if μ_R is negative. For completeness, we note that this is a specific feature of the GMSB model as, for example, in SUGRA inspired models, large trilinear couplings T_S could be present dominating this mixing.

Finally, we stress again that the finding of this section depends on the assumption that the complete flavor structure needed to explain neutrino data is present in Y_ν. If this structure is at least partially shifted to μ_S, one can reduce the predictions for the lepton flavor violating observables. It turns out that the size of this reduction depends on the SUSY parameters, and thus we do not discuss it here in detail.

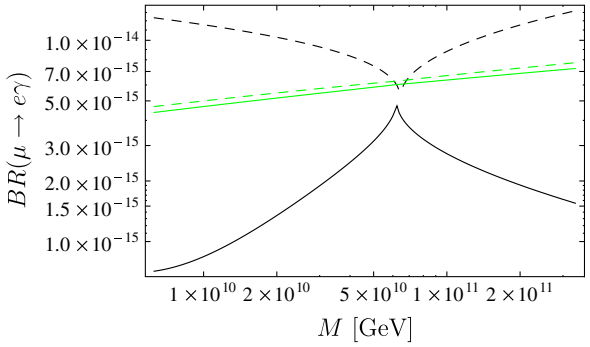

FIG. 12 (color online). Branching ratios of the LFV decay $\text{BR}(\mu \to e\gamma)$ as a function of the messenger scale M for sign $(\mu_R) = +$ (black solid line) and sign $(\mu_R) = -$ (black dashed line) fixing the other parameters as in BLRIV and $f = 0.03$. The respective straight green (light) lines show the branching ratio excluding the contribution of charged Higgsinos and sneutrinos.

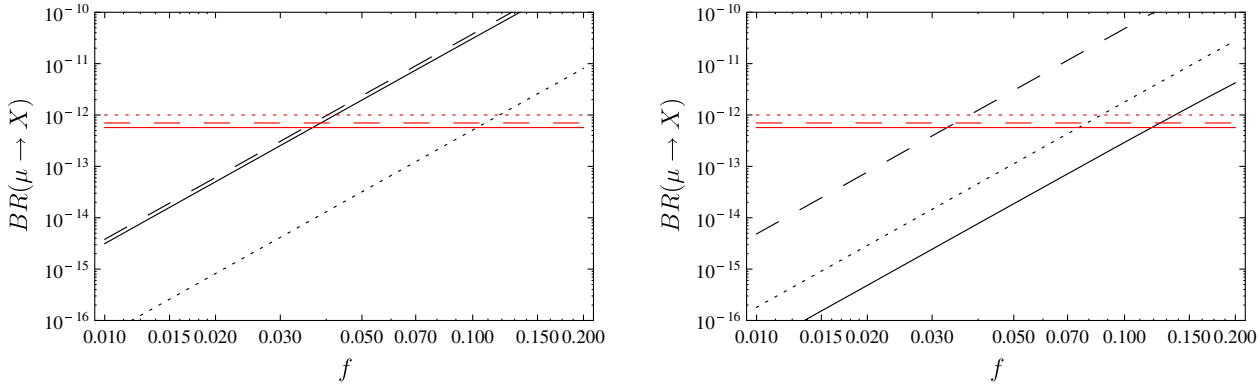

FIG. 11 (color online). Flavor violating observables as a function of f as defined in Eq. (45): $\text{BR}(\mu \to e\gamma)$ (solid line), $\text{BR}(\mu \to 3e)$ (dotted line) and $CR(\mu \to e)$ in Au (dashed line) for the points BLRI (left) and BLRIII (right) defined in Table III and using Y_ν to explain the neutrino data. The upper bounds ($\text{BR}(\mu \to e\gamma) < 5.7 \times 10^{-13}$ [137], $\text{BR}(\mu \to 3e) < 1.0 \times 10^{-12}$ [138], $CR(\mu - e, \text{Au}) < 7.0 \times 10^{-13}$ [139]) are shown as a red horizontal line, respectively.

IV. CONCLUSION

We studied in this paper the GMSB variant of a SUSY model with an extended gauge sector in which the couplings unify at the GUT scale. Compared to GMSB with MSSM particle content only, one can obtain a tree-level mass for the light doubletlike Higgs boson above M_Z, which eases the need for large radiative corrections to obtain a Higgs mass at 125 GeV. For this reason, we find in this model a lower bound on the mass of the lighter stop of about 2 TeV, which is about a factor of 2 smaller than in usual GMSB models. Nevertheless, the SUSY particles of the strongly interacting sector are rather heavy, and thus the existing bounds on squarks and gluinos are satisfied automatically. However, this implies that one needs high luminosity at the LHC with $\sqrt{s} = 14$ TeV to study this sector and the resulting cascade decays in detail. The rather heavy SUSY spectrum also implies that the rate for the doubletlike Higgs boson decaying into two photons is always below or at most the SM expectation. Therefore, this model can be ruled out if this rate turns out to be larger than the SM expectation at a significant level.

This model contains an additional candidate for the NLSP: besides the lightest neutralino or one of the sleptons, also a sneutrino can be the NLSP. For this to happen, the additional Yukawa coupling Y_S needs to have a hierarchical structure. Moreover, the stau NLSP is somewhat more difficult to achieve than in usual GMSB models. We have worked out main features of the corresponding scenarios paying also particular attention to the possiblity that the new Higgs boson, which can be rather light, can show up in the SUSY cascade decays. We have argued that Z' decays can serve as a SUSY discovery even in this rather restricted model.

Last but not least, we have discussed which lepton flavor violating observables can be observed in this class of GMSB models. It turns out that $\mu \to 3e$ and $\mu - e$-conversion are usually more constraining than $\mu \to e\gamma$. The necessary requirement for a possible observation is that there are sizable off-diagonal entries in the neutrino Yukawa coupling. It turns out that the rates for the corresponding τ decays is well below the sensitivity once the contraints from the muon sector are taken into account. Note, however, that the rates for all observables get tiny if neutrino mixings are explained via the flavor structure of μ_S instead of the flavor structure of Y_ν.

ACKNOWLEDGMENTS

We thank Martin Hirsch for useful discussions. This work has been supported by DFG Project No. PO-1337/3-1.

APPENDIX: MASS MATRICES IN THE $U(1)_R \times U(1)_{B-L}$ BASIS

Here, we give for completeness the mass matrices that were shown in the text for the original basis of $SU(3)_c \times SU(2)_L \times U(1)_R \times U(1)_{B-L}$.

1. Higgs mass matrix

In the basis $(\sigma_d, \sigma_u, \bar{\sigma}_R, \sigma_R)$, the Higgs mass matrix is given by

$$m^2_{h^0} = \begin{pmatrix} \frac{1}{4}\tilde{g}^2_{LL} v^2 c^2_\beta + m^2_A s^2_\beta & -\frac{s_{2\beta}}{8}(4m^2_A + \tilde{g}^2_{LL} v^2) & \frac{1}{4}\tilde{g}^2 v v_R c_\beta c_{\beta_R} & -\frac{1}{4}\tilde{g}^2 v v_R c_\beta s_{\beta_R} \\ -\frac{s_{2\beta}}{8}(4m^2_A + \tilde{g}^2_{LL} v^2) & \frac{1}{4}\tilde{g}^2_{LL} v^2 s^2_\beta + m^2_A c^2_\beta & -\frac{1}{4}\tilde{g}^2 v v_R s_\beta c_{\beta_R} & \frac{1}{4}\tilde{g}^2 v v_R s_\beta s_{\beta_R} \\ \frac{1}{4}\tilde{g}^2 v v_R c_\beta c_{\beta_R} & -\frac{1}{4}\tilde{g}^2 v v_R s_\beta c_{\beta_R} & \frac{1}{4}\tilde{g}^2_{RR} v^2_R c^2_{\beta_R} + m^2_{A_R} s^2_{\beta_R} & -\frac{s_{2\beta_R}}{8}(4m^2_{A_R} + \tilde{g}^2_{RR} v^2_R) \\ -\frac{1}{4}\tilde{g}^2 v v_R c_\beta s_{\beta_R} & \frac{1}{4}\tilde{g}^2 v v_R s_\beta s_{\beta_R} & -\frac{s_{2\beta_R}}{8}(4m^2_{A_R} + \tilde{g}^2_{RR} v^2_R) & \frac{1}{4}\tilde{g}^2_{RR} v^2_R s^2_{\beta_R} + m^2_{A_R} c^2_{\beta_R} \end{pmatrix}, \tag{A1}$$

where $\tilde{g}^2 = g_R(g_R - g_{BLR}) + g_{RBL}(g_{RBL} - g_{BL})$, $\tilde{g}^2_{LL} = g^2_L + g^2_R + g^2_{RBL}$, and $\tilde{g}^2_{RR} = (g_{BLR} - g_R)^2 + (g_{BL} - g_{RBL})^2$.

2. Neutralino mass matrix

The neutralino mass matrix in the basis $(\lambda_{B-L}, \lambda_{W^3}, \tilde{h}^0_d, \tilde{h}^0_u, \lambda_R, \tilde{\tilde{\chi}}_R, \tilde{\chi}_R)$ reads

$$M_{\tilde{\chi}^0} = \begin{pmatrix} M_{B-L} & 0 & -\frac{g_{RBL} v_d}{2} & \frac{g_{RBL} v_u}{2} & M_{BLR} & \frac{(g_{BL}-g_{RBL}) v_{\tilde{\chi}_R}}{2} & -\frac{(g_{BL}-g_{RBL}) v_{\chi_R}}{2} \\ 0 & M_2 & \frac{g_L v_d}{2} & -\frac{g_L v_u}{2} & 0 & 0 & 0 \\ -\frac{g_{RBL} v_d}{2} & \frac{g_L v_d}{2} & 0 & -\mu & -\frac{g_R v_d}{2} & 0 & 0 \\ \frac{g_{RBL} v_u}{2} & -\frac{g_L v_u}{2} & -\mu & 0 & \frac{g_R v_u}{2} & 0 & 0 \\ M_{BLR} & 0 & -\frac{g_R v_d}{2} & \frac{g_R v_u}{2} & M_R & -\frac{(g_R-g_{BLR}) v_{\tilde{\chi}_R}}{2} & \frac{(g_R-g_{BLR}) v_{\chi_R}}{2} \\ \frac{(g_{BL}-g_{RBL}) v_{\tilde{\chi}_R}}{2} & 0 & 0 & 0 & -\frac{(g_R-g_{BLR}) v_{\tilde{\chi}_R}}{2} & 0 & -\mu_R \\ -\frac{(g_{BL}-g_{RBL}) v_{\chi_R}}{2} & 0 & 0 & 0 & \frac{(g_R-g_{BLR}) v_{\chi_R}}{2} & -\mu_R & 0 \end{pmatrix}. \tag{A2}$$

3. Slepton mass matrix

In the basis $(\tilde{e}_L, \tilde{e}_R)$, the slepton mass matrix is given by

$$m_{\tilde{l}}^2 = \begin{pmatrix} m_{\tilde{l}L}^2 & \frac{v}{\sqrt{2}}(T_e^\dagger \cos\beta - \mu Y_e^\dagger \sin\beta) \\ \frac{v}{\sqrt{2}}(T_e \cos\beta - \mu^* Y_e \sin\beta) & m_{\tilde{l}R}^2 \end{pmatrix}, \tag{A3}$$

with

$$\begin{aligned} m_{\tilde{l}L}^2 &= m_L^2 + \frac{1}{2}v^2 \cos^2\beta Y_e^\dagger Y_e + \frac{1}{8}(-(g_L^2 - g_R g_{BLR} - g_{BL} g_{RBL})v^2 \cos 2\beta \\ &\quad - (g_{BL}^2 + g_{BLR}^2 - g_R g_{BLR} - g_{BL} g_{RBL})v_R^2 \cos 2\beta_R)\mathbf{1}, \\ m_{\tilde{l}R}^2 &= m_{e^c}^2 + \frac{1}{2}v^2 \cos^2\beta Y_e Y_e^\dagger + \frac{1}{8}(-(g_R(g_{BLR} + g_R) + g_{RBL}(g_{BL} + g_{RBL})v^2 \cos 2\beta \\ &\quad + (g_{BL}^2 - g_R^2 + g_{BLR}^2 - g_{RBL}^2)v_R^2 \cos 2\beta_R)\mathbf{1}. \end{aligned} \tag{A4}$$

4. Sneutrino mass matrix

The sneutrino mass matrix in the basis $(\tilde{\nu}, \tilde{\nu}^c, \tilde{S})$ reads

$$M_{\tilde{\nu}}^2 = \begin{pmatrix} m_{\tilde{\nu}L}^2 & \frac{v}{\sqrt{2}}(T_\nu^\dagger s_\beta - \mu Y_\nu^\dagger c_\beta) & \frac{1}{2}v v_R Y_\nu^\dagger Y_S s_\beta s_{\beta_R} \\ \frac{v}{\sqrt{2}}(T_\nu s_\beta - \mu^* Y_\nu c_\beta) & m_{\tilde{\nu}R}^2 & \frac{v_R}{\sqrt{2}}(T_S s_{\beta_R} - \mu_R^* Y_S c_{\beta_R}) \\ \frac{1}{2}v v_R Y_S^\dagger Y_\nu s_\beta s_{\beta_R} & \frac{v_R}{\sqrt{2}}(T_S^\dagger s_{\beta_R} - \mu_R Y_S^\dagger c_{\beta_R}) & m_S^2 + \frac{v_R^2 s_{\beta_R}^2}{2} Y_S^\dagger Y_S + \frac{(\mu_S^* + \mu_S^\dagger)(\mu_S + \mu_S^T)}{4} \end{pmatrix}, \tag{A5}$$

with

$$\begin{aligned} m_{\tilde{\nu}L}^2 &= m_L^2 + \frac{v^2}{2}s_\beta^2 Y_\nu^\dagger Y_\nu + \frac{1}{8}(v^2 c_{2\beta}(g_L^2 + g_R g_{BLR} + g_{BL} g_{RBL}) - v_R^2 c_{2\beta_R}(g_{BL}^2 + g_{BLR}^2 - g_R g_{BLR} - g_{BL} g_{RBL}))\mathbf{1}, \\ m_{\tilde{\nu}R}^2 &= m_{\nu^c}^2 + \frac{v_R^2}{2}s_{\beta_R}^2 Y_S Y_S^\dagger + \frac{v^2}{2}s_\beta^2 Y_\nu Y_\nu^\dagger + \frac{1}{8}(v^2 c_{2\beta}((g_R - g_{BLR})g_R + g_{RBL}(g_{RBL} - g_{BL})) \\ &\quad + v_R^2 c_{2\beta_R}((g_R - g_{BLR})^2 + (g_{BL} - g_{RBL})^2))\mathbf{1}. \end{aligned} \tag{A6}$$

[1] H. P. Nilles, Phys. Rep. **110**, 1 (1984).
[2] M. Drees, R. Godbole, and P. Roy, *Theory and Phenomenology of Sparticles: An Account of Four-Dimensional $N = 1$ Supersymmetry in High Energy Physics* (World Scientific, Singapore, 2004).
[3] M. Dine and W. Fischler, Phys. Lett. **110B**, 227 (1982).
[4] M. Dine, W. Fischler, and M. Srednicki, Nucl. Phys. **B189**, 575 (1981).
[5] S. Dimopoulos and S. Raby, Nucl. Phys. **B192**, 353 (1981).
[6] C. R. Nappi and B. A. Ovrut, Phys. Lett. **113B**, 175 (1982).
[7] L. Alvarez-Gaume, M. Claudson, and M. B. Wise, Nucl. Phys. **B207**, 96 (1982).
[8] M. Dine and A. E. Nelson, Phys. Rev. D **48**, 1277 (1993).
[9] M. Dine, R. G. Leigh, and A. Kagan, Phys. Rev. D **48**, 2214 (1993).
[10] M. Dine, A. E. Nelson, and Y. Shirman, Phys. Rev. D **51**, 1362 (1995).
[11] M. Dine, A. E. Nelson, Y. Nir, and Y. Shirman, Phys. Rev. D **53**, 2658 (1996).
[12] ATLAS Collaboration, Phys. Lett. B **710**, 49 (2012).
[13] CMS Collaboration, Phys. Lett. B **710**, 26 (2012).
[14] P. Kant, R. Harlander, L. Mihaila, and M. Steinhauser, J. High Energy Phys. 08 (2010) 104.
[15] O. Buchmueller *et al.*, Eur. Phys. J. C **72**, 1878 (2012).
[16] P. Bechtle *et al.*, J. High Energy Phys. 06 (2012) 098.
[17] O. Buchmueller *et al.*, Eur. Phys. J. C **72**, 2243 (2012).
[18] Z. Komargodski and N. Seiberg, J. High Energy Phys. 03 (2009) 072.
[19] P. Draper, P. Meade, M. Reece, and D. Shih, Phys. Rev. D **85**, 095007 (2012).

[20] Y. Shadmi and P. Z. Szabo, J. High Energy Phys. 06 (2012) 124.
[21] J. L. Evans, M. Ibe, and T. T. Yanagida, Phys. Lett. B **705**, 342 (2011).
[22] J. L. Evans, M. Ibe, S. Shirai, and T. T. Yanagida, Phys. Rev. D **85**, 095004 (2012).
[23] A. Albaid and K. Babu, arXiv:1207.1014.
[24] M. Abdullah, I. Galon, Y. Shadmi, and Y. Shirman, arXiv:1209.4904.
[25] N. Craig, S. Knapen, D. Shih, and Y. Zhao, J. High Energy Phys. 03 (2013) 154.
[26] J. A. Evans and D. Shih, arXiv:1303.0228.
[27] I. Donkin and A. K. Knochel, arXiv:1205.5515.
[28] P. Byakti and T. S. Ray, J. High Energy Phys. 05 (2013) 055.
[29] P. Grajek, A. Mariotti, and D. Redigolo, arXiv:1303.0870.
[30] M. Maniatis, Int. J. Mod. Phys. A **25**, 3505 (2010).
[31] U. Ellwanger, C. Hugonie, and A. M. Teixeira, Phys. Rep. **496**, 1 (2010).
[32] U. Ellwanger and C. Hugonie, Mod. Phys. Lett. A **22**, 1581 (2007).
[33] U. Ellwanger, J. High Energy Phys. 03 (2012) 044.
[34] J. F. Gunion, Y. Jiang, and S. Kraml, Phys. Lett. B **710**, 454 (2012).
[35] G. G. Ross, K. Schmidt-Hoberg, and F. Staub, J. High Energy Phys. 08 (2012) 074.
[36] K. Benakli, M. D. Goodsell, and F. Staub, arXiv:1211.0552.
[37] M. Carena, S. Gori, N. R. Shah, and C. E. Wagner, J. High Energy Phys. 03 (2012) 014.
[38] R. Benbrik, M. Gomez Bock, S. Heinemeyer, O. Stål, G. Weiglein, and L. Zeune, Eur. Phys. J. C **72**, 2171 (2012).
[39] K. Schmidt-Hoberg and F. Staub, J. High Energy Phys. 10 (2012) 195.
[40] S. F. King, M. Muhlleitner, R. Nevzorov, and K. Walz, Nucl. Phys. **B870**, 323 (2013).
[41] K. Schmidt-Hoberg, F. Staub, and M. W. Winkler, J. High Energy Phys. 01 (2013) 124.
[42] Z. Heng, arXiv:1210.3751.
[43] J.-J. Cao, Z.-X. Heng, J. M. Yang, Y.-M. Zhang, and J.-Y. Zhu, J. High Energy Phys. 03 (2012) 086.
[44] M. Cvetic and J. C. Pati, Phys. Lett. **135B**, 57 (1984).
[45] M. Cvetic and P. Langacker, arXiv:hep-ph/9707451.
[46] C. S. Aulakh, K. Benakli, and G. Senjanovic, Phys. Rev. Lett. **79**, 2188 (1997).
[47] C. S. Aulakh, A. Melfo, A. Rasin, and G. Senjanovic, Phys. Rev. D **58**, 115007 (1998).
[48] P. Fileviez Perez and S. Spinner, Phys. Lett. B **673**, 251 (2009).
[49] F. Siringo, Eur. Phys. J. C **32**, 555 (2004).
[50] H. E. Haber and M. Sher, Phys. Rev. D **35**, 2206 (1987).
[51] M. Drees, Phys. Rev. D **35**, 2910 (1987).
[52] M. Cvetic, D. A. Demir, J. R. Espinosa, L. L. Everett, and P. Langacker, Phys. Rev. D **56**, 2861 (1997).
[53] S. Nie and M. Sher, Phys. Rev. D **64**, 073015 (2001).
[54] E. Ma, Phys. Lett. B **705**, 320 (2011).
[55] M. Hirsch, M. Malinsky, W. Porod, L. Reichert, and F. Staub, J. High Energy Phys. 02 (2012) 084.
[56] P. Minkowski, Phys. Lett. **67B**, 421 (1977).
[57] T. Yanagida, Conf. Proc. **C7902131**, 95 (1979).
[58] R. N. Mohapatra and G. Senjanovic, Phys. Rev. Lett. **44**, 912 (1980).
[59] J. Schechter and J. W. F. Valle, Phys. Rev. D **22**, 2227 (1980).
[60] S. Bertolini, L. Di Luzio, and M. Malinsky, Phys. Rev. D **80**, 015013 (2009).
[61] V. De Romeri and M. Hirsch, J. High Energy Phys. 12 (2012) 106.
[62] L. Basso, A. Belyaev, D. Chowdhury, M. Hirsch, S. Khalil, S. Moretti, B. O'Leary, W. Porod, and F. Staub, Comput. Phys. Commun. **184**, 698 (2013).
[63] M. Malinsky, J. C. Romao, and J. W. F. Valle, Phys. Rev. Lett. **95**, 161801 (2005).
[64] V. De Romeri, M. Hirsch, and M. Malinsky, Phys. Rev. D **84**, 053012 (2011).
[65] T. Aaltonen *et al.* (CDF Collaboration), Phys. Rev. Lett. **106**, 121801 (2011).
[66] V. M. Abazov *et al.* (D0 Collaboration), Phys. Lett. B **695**, 88 (2011).
[67] ATLAS Collaboration, Phys. Rev. Lett. **107**, 272002 (2011).
[68] CMS Collaboration, J. High Energy Phys. 05 (2011) 093.
[69] A. Leike, Phys. Rep. **317**, 143 (1999).
[70] P. Langacker, Rev. Mod. Phys. **81**, 1199 (2009).
[71] B. Holdom, Phys. Lett. **166B**, 196 (1986).
[72] K. S. Babu, C. Kolda, and J. March-Russell, Phys. Rev. D **57**, 6788 (1998).
[73] F. del Aguila, G. D. Coughlan, and M. Quiros, Nucl. Phys. **B307**, 633 (1988).
[74] T. G. Rizzo, Phys. Rev. D **59**, 015020 (1998).
[75] T. G. Rizzo, Phys. Rev. D **85**, 055010 (2012).
[76] M. E. Krauss, B. O'Leary, W. Porod, and F. Staub, Phys. Rev. D **86**, 055017 (2012).
[77] B. O'Leary, W. Porod, and F. Staub, J. High Energy Phys. 05 (2012) 042.
[78] Y. Mambrini, J. Cosmol. Astropart. Phys. 07 (2011) 009.
[79] L. Basso, B. O'Leary, W. Porod, and F. Staub, J. High Energy Phys. 09 (2012) 054.
[80] M. Hirsch, L. Reichert, W. Porod, and F. Staub, Phys. Rev. D **86**, 093018 (2012).
[81] P. S. Bhupal Dev and R. N. Mohapatra, Phys. Rev. D **81**, 013001 (2010).
[82] P. S. Bhupal Dev and R. N. Mohapatra, Phys. Rev. D **82**, 035014 (2010).
[83] L. E. Ibanez and G. G. Ross, Phys. Lett. B **260**, 291 (1991).
[84] H. K. Dreiner, C. Luhn, and M. Thormeier, Phys. Rev. D **73**, 075007 (2006).
[85] R. M. Fonseca, M. Malinsky, W. Porod, and F. Staub, Nucl. Phys. **B854**, 28 (2012).
[86] G. Giudice and R. Rattazzi, Nucl. Phys. **B511**, 25 (1998).
[87] G. Giudice and R. Rattazzi, Phys. Rep. **322**, 419 (1999).
[88] S. P. Martin, Phys. Rev. D **55**, 3177 (1997).
[89] N. Arkani-Hamed, G. F. Giudice, M. A. Luty, and R. Rattazzi, Phys. Rev. D **58**, 115005 (1998).
[90] G. Giudice and A. Masiero, Phys. Lett. B **206**, 480 (1988).
[91] M. A. Ajaib, I. Gogoladze, F. Nasir, and Q. Shafi, Phys. Lett. B **713**, 462 (2012).
[92] F. Brummer, S. Kraml, and S. Kulkarni, J. High Energy Phys. 08 (2012) 089.

[93] S. Dimopoulos, G. Giudice, and A. Pomarol, Phys. Lett. B **389**, 37 (1996).
[94] M. Fujii and T. Yanagida, Phys. Rev. D **66**, 123515 (2002).
[95] K. Jedamzik, M. Lemoine, and G. Moultaka, Phys. Rev. D **73**, 043514 (2006).
[96] M. Viel, J. Lesgourgues, M. G. Haehnelt, S. Matarrese, and A. Riotto, Phys. Rev. D **71**, 063534 (2005).
[97] A. Boyarsky, J. Lesgourgues, O. Ruchayskiy, and M. Viel, J. Cosmol. Astropart. Phys. 05 (2009) 012.
[98] E. A. Baltz and H. Murayama, J. High Energy Phys. 05 (2003) 067.
[99] M. Fujii and T. Yanagida, Phys. Lett. B **549**, 273 (2002).
[100] M. Lemoine, G. Moultaka, and K. Jedamzik, Phys. Lett. B **645**, 222 (2007).
[101] F. Staub, W. Porod, and J. Niemeyer, J. High Energy Phys. 01 (2010) 058.
[102] J. Hasenkamp and J. Kersten, Phys. Rev. D **82**, 115029 (2010).
[103] K. Kamada, Y. Nakai, and M. Sakai, Prog. Theor. Phys. **126**, 35 (2011).
[104] K. Choi, K. Hwang, H. B. Kim, and T. Lee, Phys. Lett. B **467**, 211 (1999).
[105] F. Staub, arXiv:0806.0538.
[106] F. Staub, Comput. Phys. Commun. **181**, 1077 (2010).
[107] F. Staub, Comput. Phys. Commun. **182**, 808 (2011).
[108] F. Staub, Comput. Phys. Commun. **184**, 1792 (2013).
[109] W. Porod, Comput. Phys. Commun. **153**, 275 (2003).
[110] W. Porod and F. Staub, Comput. Phys. Commun. **183**, 2458 (2012).
[111] A. Dedes, G. Degrassi, and P. Slavich, Nucl. Phys. **B672**, 144 (2003).
[112] A. Brignole, G. Degrassi, P. Slavich, and F. Zwirner, Nucl. Phys. **B643**, 79 (2002).
[113] A. Brignole, G. Degrassi, P. Slavich, and F. Zwirner, Nucl. Phys. **B631**, 195 (2002).
[114] G. Degrassi, P. Slavich, and F. Zwirner, Nucl. Phys. **B611**, 403 (2001).
[115] H. Dreiner, K. Nickel, W. Porod, and F. Staub, arXiv:1212.5074.
[116] E. Accomando *et al.* (CLIC Physics Working Group), arXiv:hep-ph/0412251.
[117] L. Linssen, A. Miyamoto, M. Stanitzki, and H. Weerts, arXiv:1202.5940.
[118] ATLAS Collaboration, Phys. Lett. B **716**, 1 (2012).
[119] CMS Collaboration, Phys. Lett. B **716**, 30 (2012).
[120] ATLAS Collaboration, BEH detection to boson pairs in ATLAS, Rencontres de Moriond, 2013.
[121] L. Basso and F. Staub, Phys. Rev. D **87**, 015011 (2013).
[122] CMS Collaboration, Report No. CMS PAS HIG-13-001.
[123] J. L. Feng and T. Moroi, Phys. Rev. D **58**, 035001 (1998).
[124] M. Drees and X. Tata, Phys. Lett. B **252**, 695 (1990).
[125] ATLAS Collaboration, Phys. Lett. B **720**, 277 (2013).
[126] ATLAS collaboration, Report No. ATLAS-CONF-2013-017.
[127] CMS Collaboration, Report No. CMS PAS EXO-12-061.
[128] A. Belyaev, N. D. Christensen, and A. Pukhov, Comput. Phys. Commun. **184**, 1729 (2013).
[129] F. Staub, T. Ohl, W. Porod, and C. Speckner, Comput. Phys. Commun. **183**, 2165 (2012).
[130] C.-F. Chang, K. Cheung, and T.-C. Yuan, J. High Energy Phys. 09 (2011) 058.
[131] G. Corcella and S. Gentile, Nucl. Phys. **B866**, 293 (2013).
[132] T. Gherghetta, T. A. Kaeding, and G. L. Kane, Phys. Rev. D **57**, 3178 (1998).
[133] J. Kang and P. Langacker, Phys. Rev. D **71**, 035014 (2005).
[134] M. Baumgart, T. Hartman, C. Kilic, and L.-T. Wang, J. High Energy Phys. 11 (2007) 084.
[135] R. N. Mohapatra and J. W. F. Valle, Phys. Rev. D **34**, 1642 (1986).
[136] M. Gonzalez-Garcia, M. Maltoni, J. Salvado, and T. Schwetz, J. High Energy Phys. 12 (2012) 123.
[137] J. Adam *et al.* (MEG Collaboration), arXiv:1303.0754.
[138] J. Beringer *et al.* (Particle Data Group), Phys. Rev. D **86**, 010001 (2012).
[139] W. H. Bertl *et al.* (SUNDRUM II Collaboration), Eur. Phys. J. C **47**, 337 (2006).
[140] M. Hirsch, F. Staub, and A. Vicente, Phys. Rev. D **85**, 113013 (2012).
[141] A. Abada, D. Das, A. Vicente, and C. Weiland, J. High Energy Phys. 09 (2012) 015.
[142] A. Ilakovac, A. Pilaftsis, and L. Popov, Phys. Rev. D **87**, 053014 (2013).